



UNIVERSITAT
POLITÈCNICA
DE VALÈNCIA



UNIVERSITAT POLITÈCNICA DE VALÈNCIA

Escuela Técnica Superior de Ingeniería Industrial

Desarrollo y puesta a punto de una instalación
experimental para caracterizar el proceso de inyección de
Amoniaco a partir de la cantidad de Movimiento

Trabajo Fin de Grado

Grado en Ingeniería en Tecnologías Industriales

AUTOR/A: Cheddadi Rouchi, Omar

Tutor/a: Bracho León, Gabriela Cristina

CURSO ACADÉMICO: 2023/2024

Executive summary.

CONCEPT (ABET)	Accomplished?	Where?
1. IDENTIFY		
1.1. Problem statement and opportunity.	YES	2, 7, 8, 21
1.2. Constraints (standards, codes, needs, requirements & specifications).	YES	15, 23, 37, 41
1.3. Setting goals.	YES	8, 34
2. FORMULATE:		
2.1. Creative solution generation (analysis).	YES	37, 44
2.2. Evaluation of multiple solutions and decision-making (synthesis).	YES	37-45
3. SOLVE:		
3.1. Fulfillment goals.	YES	59-71
3.2. Overall impact and significance (contributions and practical recommendations)	YES	64-71

Summary

This project investigates the potential of ammonia as a sustainable fuel alternative for maritime applications, focusing on the re-design and adaptation of a momentum flux test rig to accommodate ammonia's properties. The study aims to address global warming by developing clean energy solutions that align with the United Nations Sustainable Development Goals (SDGs), particularly SDG 7 (Affordable and Clean Energy), SDG 13 (Climate Action), and SDG 14 (Life Below Water). The research involves the analysis of ammonia's injection characteristics compared to diesel, evaluating its feasibility as a substitute in internal combustion engines (ICEs). Modifications to the test rig, including the adaptation of gaskets, pipes, and the discharge system, were necessary to ensure compatibility with ammonia's corrosive and toxic properties. The experimental setup proved effective, demonstrating that ammonia can exhibit stable injection characteristics similar to diesel. This study lays the groundwork for further exploration of ammonia dynamics and its potential role in decarbonizing the transport and energy sectors.

The results suggest that with appropriate technology, ammonia can replace diesel without significant performance loss, highlighting the importance of continued research and development in this field. Future work will focus on enhancing the test rig's capabilities, characterizing injector hydraulics, and developing correlation algorithms for injection rates, thereby contributing to the broader goal of reducing greenhouse gas emissions and mitigating climate change.

Acknowledgements

First and foremost, I would like to express my gratitude to Dr. Gabriela Bracho for giving me the opportunity to work alongside her on this project. Her invaluable guidance and support throughout this process have been crucial to its completion. I am also grateful to Daniel Pinilla for his collaboration and assistance.

I dedicate this project to my parents, who have always encouraged my growth and reminded me of the value of education. I distinctly remember the joy on their faces when I first got admitted to university four years ago. I hope to recreate that moment of pride once again, now with a greater sense of accomplishment as I graduate. To my sisters, my biggest cheerleaders, thank you for your unwavering support and for always being there for me. I would not be where I am today without your unconditional love and encouragement.

To my best friends, Andrea, Laura, and Irene, thank you for the countless days and nights spent studying together in the library, the spontaneous trips, and the endless words of encouragement. A special mention goes to Javier and Jorge; thank you for always providing a shoulder to lean on, for sharing these past four years of living together, and for picking me back up when I could no longer keep going.

Lastly, to my eighteen-year-old self, who left his family behind to move to Valencia, questioning if this degree was really for him after failing the first midterms – I hope I have made you proud.

*“To the class of 2024 in Gaza, whose lives have been tragically taken from them,
who worked so hard for their future, a future denied to them by the relentless
shadow of Israeli occupation.”*

Table of Contents

List of Tables	IX
List of Figures	X
I PROJECT REPORT	1
1 Introduction	2
1.1 Global warming.	2
1.2 International deals and SDGs.	5
1.3 Transport sector impact on the environment.	7
1.4 Objectives of the research.	8
1.5 About the Clean Mobility & Thermofluids Institute.	9
1.6 Justification	10
2 Literature Review	11
2.1 State of the art technology in ICEs. Use of alternative fuels.	11

2.2	Ammonia.	13
2.2.1	Ammonia as an energy vector.	13
2.2.2	Properties of ammonia.	15
2.2.3	Emissions.	17
2.2.4	Hazards of storage and manipulation of ammonia.	19
2.2.5	Alignment with the SDGs.	20
2.3	Research and state of the art technology on NH ₃ fuelled ICEs. . . .	21
2.4	Regulations.	23
2.5	Fuel injection system.	24
2.5.1	Common rail direct injection.	24
2.5.2	The injector.	25
2.5.3	How much may ammonia differ from diesel in injection. . . .	27
2.6	Momentum flux. Definition, utility and experimental measurement technique.	29
3	Re-design of the test-rig and set-up of the experimental installation.	33
3.1	Starting point. Available momentum flux test-rig.	34
3.2	Description and justification of the modifications made to adapt the test-rig to ammonia conditions.	37
3.2.1	Gaskets.	37
3.2.2	Injector holder.	41

3.2.3	Sensor holder.	42
3.2.4	Fuel return collector sleeve.	44
3.2.5	Re-designed assembly.	45
3.3	Set-up of the experimental installation.	46
3.3.1	Mechanical Installation	46
3.3.2	Electric Installation	49
3.4	Experimental installation.	51
4	Methodology.	52
4.1	Software employed.	52
4.2	Momentum flux signal obtention.	56
4.3	Cumulative phenomena.	57
4.4	Testing plan.	58
5	Results and Discussion.	59
5.1	Base case. Diesel as fuel.	59
5.2	Ammonia as fuel.	61
5.3	Parametric analysis.	62
5.4	Further analysis of the results.	64
5.5	Rate of injection inference from momentum flux measurements.	66
5.5.1	Base case.	67
5.5.2	Ammonia rate of injection.	68

6	Conclusions and further development.	70
6.1	Conclusions.	70
6.2	Further developments.	71
	Bibliography	73
II	TERMS OF REFERENCE	79
7	General Conditions of the Injection Laboratory.	80
7.1	Experimental room conditions.	80
7.2	Installation conditions.	81
7.3	Rules for operators.	82
7.4	Recommendations for nitrogen use.	82
7.5	Recommendations for ammonia use.	82
8	Methodology for using the installation	83
8.1	Start-up and shut-down sequences.	83
9	Installation maintenance.	86
9.1	Daily maintenance.	86
9.2	Periodic maintenance.	87

III BUDGET	88
10 BUDGET	89
IV DRAWINGS	91

List of Tables

2.1	Fuel properties comparison. Compiled from [31]&[32]	15
3.1	Table of ordered o-rings.	38
4.1	Testing plan matrix.	58
5.1	Diesel ROI and momentum flux data.	68
5.2	Diesel results.	68
5.3	Ammonia momentum flux data.	69
5.4	Ammonia results.	69

List of Figures

1.1	Temperature and atmospheric C_{O_2} concentrations over the past 800 thousand years [2].	3
1.2	Global mean temperature difference, compared to the 1850-1900 baseline, for the five major global climate datasets[3].	4
1.3	Carbon dioxide emissions scenarios to limit global warming to 1.5°C.[8]	4
1.4	UN Sustainable Development Goals[13]	6
1.5	CO_2 emissions by sector [15].	7
2.1	Cost estimate for ammonia and hydrogen transportation by principal modes of transport [27].	13
2.2	Ammonia production and use cycle. (Adapted from [29])	14
2.3	Selective catalytic reduction process. [35]	17
2.4	Common rail injection system diagram [50].	24
2.5	Diesel injector diagram [51].	25
2.6	Operation of a common rail injector [18].	26
2.7	Vapor and liquid spray penetration evolution for diesel and ammonia [52].	27

2.8	Definition of effective area and velocity [18].	30
2.9	Measuring principle of momentum flux. Adapted from [18].	32
3.1	Front view of available test-rig.	34
3.2	Cross section of available test-rig.	35
3.3	Refrigerated injector holder cross section.	36
3.4	Indirect measurement of o-ring groove dimensions.	37
3.5	O-ring diameters definition.	38
3.6	Exploded view of gaskets in the test-rig.	39
3.7	Teflon gasket close-up view.	40
3.8	Angled injector holder.	41
3.9	Straight injector holder.	41
3.10	Angled sensor holder.	42
3.11	Straight sensor holder.	42
3.12	Exploded view of sensor holder assembly.	42
3.13	Sensor configuration view on the test-rig.	43
3.14	Modeled and actual nozzle-sensor view.	43
3.15	Return sleeve model.	44
3.16	Return sleeve model and actual assembly.	44
3.17	Modified test-rig model for ammonia.	45
3.19	Injector.	46

3.18	Experimental installation diagram.	47
3.20	Close up view on the refrigeration circuit and the return sleeve. . .	48
3.21	Electronic system diagram.	49
3.22	YOKOGAWA digital scope.	50
3.23	Experimental installation.	51
4.1	Excel datasheet.	52
4.2	ICU controller.	53
4.3	YOKO DL716 software.	53
4.4	Xtasutiles in MATLAB.	54
4.5	Pump controller.	54
4.6	Temperature recorder.	55
4.7	50 momentum flux signals.	56
4.8	Average signal.	56
4.9	Cumulative phenomena [55].	57
4.10	Signal correction [55].	57
5.1	Rate of injection vs momentum flux signals for diesel of both injectors.	60
5.2	Momentum flux signals of diesel for both injectors.	60
5.3	Momentum flux signals of ammonia for both injectors.	61
5.4	Momentum flux signals for 250 μ m injector of diesel and NH ₃	62
5.5	Momentum flux signals for 300 μ m injector of diesel and NH ₃	63

5.6	Overlaid momentum flux signals of diesel and ammonia.	64
5.7	Rate of penetration.	65
5.8	Momentum flux signals.	65
5.9	ROI and momentum flux signals for diesel.	67
5.10	Momentum flux signals of two different operation points with ammonia.	68

Part I

PROJECT REPORT

Chapter 1

Introduction

1.1 Global warming.

Earth's climate has changed throughout history. Most of the changes are attributed to fluctuations in the planet orbital path, known as Milankovitch Cycles[1]. These cycles influence the amount of solar energy received by the planet. However, this framework does not provide grounds for understanding all of the changes that occurred through the millennia, let alone the substantially short period of rapid warming Earth has experienced since the Industrial Revolution. Scientists are confident this recent warming is primarily due to human emissions of greenhouse gases (GHG) into Earth's atmosphere from burning fossil fuels[1].

Figure 1.1 is based on the comparison of atmospheric samples contained in ice cores and more recent direct measurements. It provides evidence that atmospheric CO₂ has increased since the Industrial Revolution [2].

Greenhouse gases allow the influx of solar radiation into the atmosphere, but then impede heat radiation reflected on the surface of the planet from escaping back to outer space[3]. The Industrial Revolution, which began in the late 18th century, was initially characterized by the use of hand-powered machines. Subsequently, the burning of organic materials was incorporated as a source of energy.

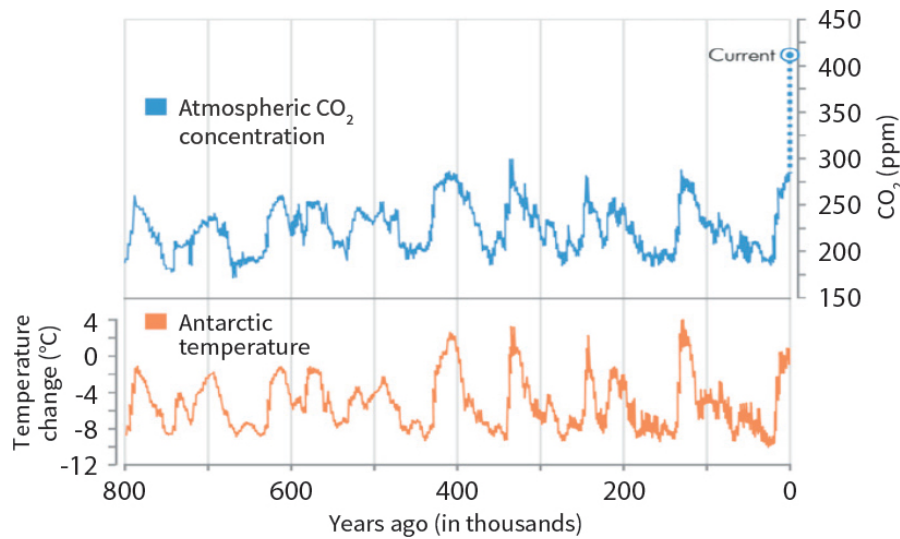


Figure 1.1: Temperature and atmospheric CO₂ concentrations over the past 800 thousand years [2].

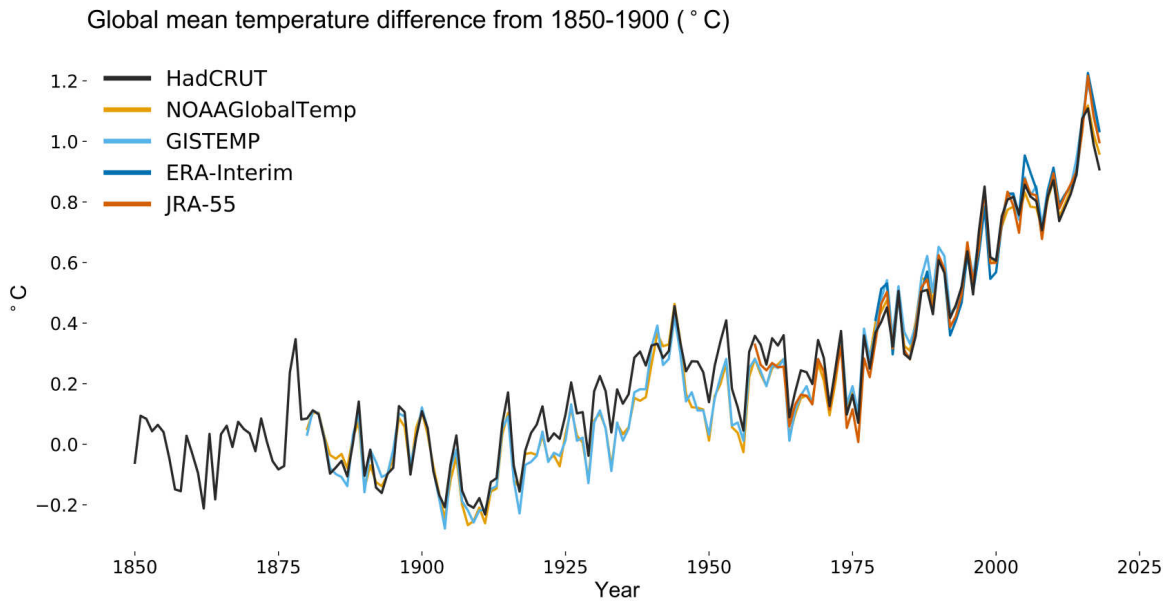
Finally, fossil fuels became the main source of energy, driving large-scale industrialization, resulting in a substantial increase of the levels of carbon dioxide, methane, nitrous oxides and halogenated gases (CFCs), which accentuated the greenhouse effect, leading to the raise of the planet average temperature and the consequent climate change effects [4][5].

Carbon dioxide is a potent GHG that, once it reaches the atmosphere, remains and affects the climate system in the long term, up to thousands of years [4]. Thus, the main concern is to mitigate these emissions, with the final goal of reaching global net-zero GHG emissions by 2050 [6].

The shared goal is to stabilise the global temperature at a level not above 1,5°C increase compared with pre-industrial values, mitigating in this way a temperature overshoot. As we can see in figure 1.2, the increase in temperature trend is obvious, which coincide with the increment of GHG emissions.

Immediate action by the international community is required, the projected 2°C threshold for year 2100 could be surpassed before 2032 [7] if greenhouse gas concentrations are not reduced. The next years will be decisive. If action is delayed, an even faster pace of transition will be required and thus the transition will likely be more disorderly. (See figure 1.3)[8].

Met Office



© Crown Copyright. Source: Met Office

Figure 1.2: Global mean temperature difference, compared to the 1850-1900 baseline, for the five major global climate datasets[3].

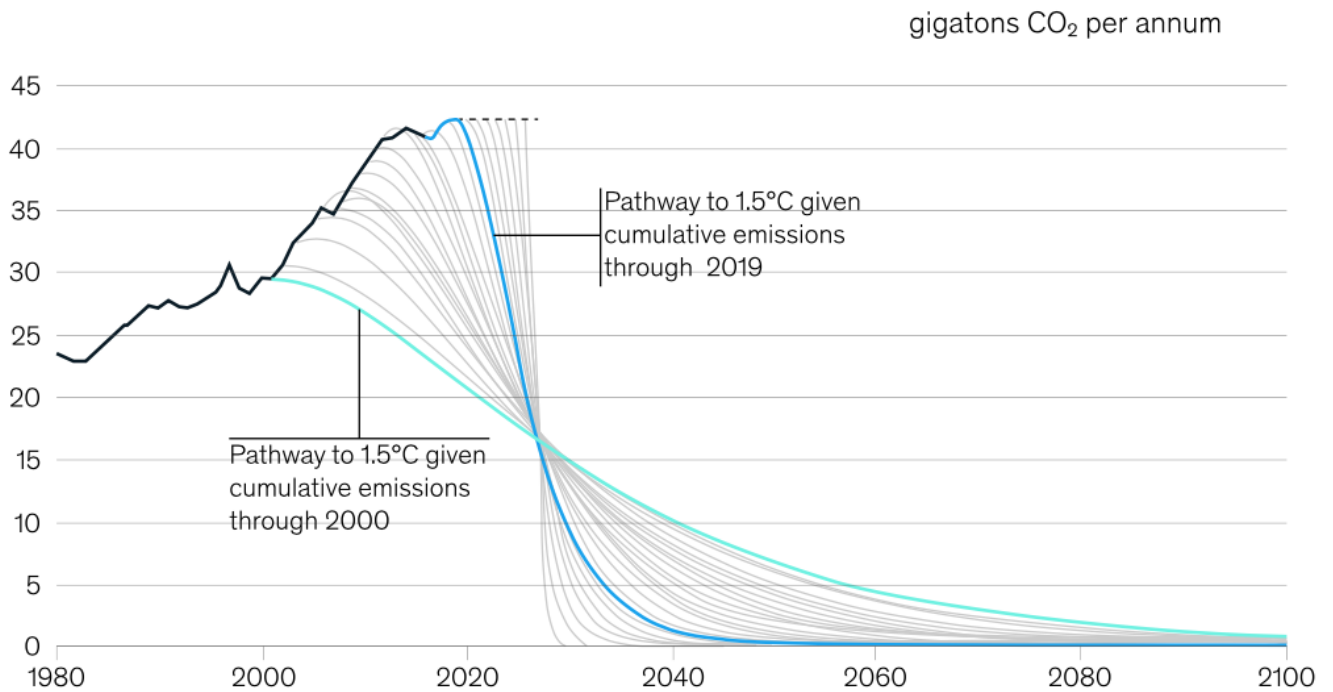


Figure 1.3: Carbon dioxide emissions scenarios to limit global warming to 1.5°C.[8]

1.2 International deals and SDGs.

Climate change poses a significant threat to the future, demanding unified global action. International legislation and agreements have become vital tools in guiding countries to curb greenhouse gas emissions and mitigate the impact on the environment.

The United Nations Framework Convention on Climate Change (UNFCCC) was adopted in the nineties, key agreements like the Kyoto Protocol and the Paris Agreement were built on the Convention.

The Kyoto Protocol [9], adopted in 1997 and in force since 2005, was the first major international agreement to establish binding greenhouse gas emission reduction targets for industrialised countries. The aim was to reduce the emissions to 5,2 per cent below 1990 levels from 2008 to 2012. In 2012, at COP18, delegates agreed to extend the Protocol until 2020.

In 2015, after a series of conferences marked by disagreements, a new legally binding agreement was signed at COP21, held in Paris. The Paris Agreement [10] pledges to limit the increase of the world's temperature to 2°C above pre-industrial levels, and pursue efforts to limit it to 1,5°C, by the end of the century. This replaced the Kyoto Protocol after entering into force in 2016. Another objective is to reach net-zero emissions by 2050, this refers to the balance between the amount of GHG that is produced and the amount that is removed from the atmosphere [11].

On a regional level, various agreements and policies complement global initiatives. For example, the European Union has rolled out a comprehensive set of measures aimed at reducing emissions, including an emissions trading system and initiatives to promote renewable energy sources[12].

Importantly, these legislative measures and international agreements not only set binding commitments for countries but also create a supportive environment for investment in clean technologies and innovation. By providing a clear and consistent framework for action, they encourage businesses and institutions to develop sustainable solutions to combat climate change.

Implementation of the agreements is essential for the achievement of the Sustainable Development Goals (SDGs).

SDGs are a blueprint for collective action by all countries, adopted by UN member

states in 2015 as part of the 2030 Agenda for sustainable development. This ambitious agenda recognizes and tackles pressing social, economic, and environmental issues facing the Earth.

Developed through years of collaboration between the United Nations (UN) and its member states, the 17 SDGs [13] build upon past and current international agreements.

The 17 SDGs are further broken down into 169 specific targets, providing measurable steps to track progress. With a deadline of 2030 for achieving these goals, the urgency of collective action is clear.



Figure 1.4: UN Sustainable Development Goals[13]

This project addresses critical aspects of the following SDGs:

- SDG 7: Affordable and Clean Energy.** The research contributes to this goal by developing a sustainable fuel alternative for the maritime industry. This could potentially lead to a cleaner and more affordable energy source for ships, reducing reliance on traditional fossil fuels.
- SDG 13: Climate Action.** The project focuses on GHG reduction in maritime transport. By developing a sustainable fuel, the aim is to decrease the industry’s overall carbon footprint and contribute to mitigating climate change.
- SDG 14: Life Below Water.** Traditional maritime fuels can be harmful to marine ecosystems through spills. Additionally, by reducing greenhouse gas emissions, we will preserve the health of the oceans.

1.3 Transport sector impact on the environment.

Transport is a vital sector, but our current mobility system is not efficient. Being one of the pillars of modern societies, contributing to a better quality of life, it helps to boost the economy and reach remote areas, it is also responsible of about a quarter of the European Union GHG emissions [14].

As demand increases, so has the overall energy efficiency of the sector. However, the global transport emissions did not decrease at the same pace [15]. We can see in figure 1.5 that the volume of CO₂ has been steadily over the last decades.

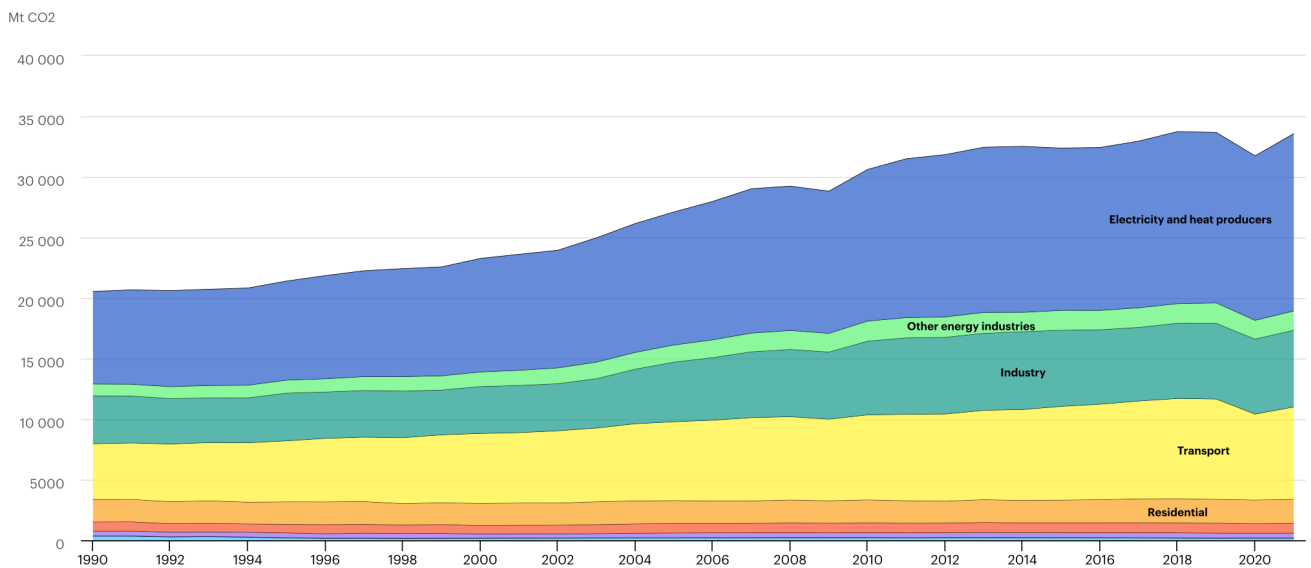


Figure 1.5: CO₂ emissions by sector [15].

The sector has a strong reliance on fossil fuels, this only negligible amounts of renewable fuels in use. For road-based transport electrification is expected to cut down in half the global emissions by 2050 [16], however, long-distance journeys in shipping and aviation not rely on direct electrification or significant emissions reduction. Both modes depend on low-carbon fuels with comparable energy densities to incumbent fossil fuels counterparts [17].

In this project, the focus is on ammonia. It can be produced through an industrial process converting electric energy into chemical energy. Ammonia does not produce direct CO₂ emissions when burning in an ICE, therefore, it is a feasible candidate for substituting fossil fuels in the marine sector.

1.4 Objectives of the research.

The main objective of this project is to characterize the hydraulic behaviour of a high-injection system operating with ammonia. The experimental characterization is based on the momentum flux measurement of the ammonia spray. This experimental technique has been widely used in the past for conventional fossil fuels, but this is the first time that it will be implemented for a carbon-free fuel. The use of NH_3 has some challenges due to some properties of the fluid that differ from conventional fuels.

To fulfill the main goal, the following partial objectives have been described:

- PO1 Re-design of the spray momentum flux test rig.** At the CMT facilities, there is an existing test rig that was designed for diesel applications [18]. Due to the corrosive and toxic characteristics of NH_3 , this test rig must be adapted. Therefore, some parts, coupling connectors, pipes, washers, o-rings, etc... are re-designed to guarantee a safe operation of the system.
- PO2 Measurement of the momentum flux of ammonia.** Once the test rig is ready, the momentum flux measurements will be carried out considering operating conditions that resemble the chamber pressure and gas density in an engine. Different configurations of injection pressure and back pressure will be tested. The same test plan must be conducted employing diesel. This measurements will be useful for establishing a common ground to compare and analyse the results, since diesel is an extensively studied fuel.
- PO3 Analysis of the results.** The resulting data from the experiments will be processed. This will allow to generate graphs and tables. By analysing the data obtained, the aim is to identify behavioural correlations between the two fuels. This will shed light on the understanding of ammonia behaviour in ICEs.

1.5 About the Clean Mobility & Thermofluids Institute.

The CMT – Clean Mobility and Thermofluids is a research and educational centre actively engaged in the research and development of Applied Thermo-Fluid Science. With over 40 years of experience, it conducts applied studies to optimize industrial systems' behaviour and aid in their development, alongside basic research aimed at enhancing understanding of relevant physical processes. The centre maintains strong relationships with prominent figures in the transportation and energy sectors, both nationally and internationally, including Stellantis, Stadler, Volvo, Wärtsilä, Aramco, and others.

The centre stands out as one of the few research facilities in Spain actively involved in injection and alternative fuels research. Equipped with specialized tools, it can measure various parameters such as injection rate, jet opening angle, and liquid jet length, among others. These measurements are conducted under diverse operating conditions, including variations in nozzle diameter, backpressure, and temperature.

Regarding the use of ammonia as a fuel, the CMT is at the forefront of research, collaborating closely with institutions such as Politecnico di Milano. Despite the relatively short duration of this research, significant advancements have already been made in this field [19].

1.6 Justification

This research falls within the scope of the work package WP TED2021-129379A-I00 of the national project DIGIAMMONIA funded by the Spanish Ministry of Science and Innovation and the European Union “NextGenerationEU”/PRTR. The overall project aims to understand the injection-combustion process to promote sustainable and digital transport technologies and to support alternative fuels for propulsive systems in the maritime sector.

The project tries to understand the potential of ammonia and O₂-enriched air combustion, constituting a source of scientific and technological results on the field of sustainable fuels and decarbonisation for the new generation of propulsion systems.

By measuring the momentum flux of the spray, we can indirectly obtain the injection rate of ammonia, which is crucial for the quantification of spray evolution in any kind of predictive model. This thesis addresses this gap by acquiring factual data on ammonia injection, crucial for developing a more accurate 1D and 3D spray models, specifically for ammonia as a fuel. Existing research relies on diesel-like models, potentially leading to misleading results. Since we lack factual data to confirm a strong correlation between ammonia and diesel behavior, extrapolating results from diesel models can be inaccurate.

Hence, the development of this research aims to close the gap in the literature and to have a broader understanding of ammonia as a fuel.

Chapter 2

Literature Review

2.1 State of the art technology in ICEs. Use of alternative fuels.

Internal combustion engines (ICE) operating on fossil fuels provide about 25% of the world's power [20]. Reducing emissions, fuel consumption and reaching higher efficiency has been the goal of researchers and manufacturers for years. Today's ICEs are a marvel of engineering, thanks to significant advancements on the field.

For light duty engines, technologies such as start/stop, variable compression ratio and active cylinder deactivation drop fuel consumption up to 20% from the gasoline direct injection baseline.

Lean NO_x control has also improved substantially. Thermal durability of selective catalytic reduction (SCR) catalysts has reached peak performance, being SCR filters able to meet EU requirements, showing remarkable ammonia nitrates inhibition capacity. In combination with the implementation of catalyzed soot filters, the overall emissions of ICE is at the lowest point [21].

In the future the combustion engine will play a central role, even though mobility will be characterized by a shift to battery and hybrid electric vehicles, fuel cell vehicles and conventional engines will still be in use. Power generation and heavy duty machines will strongly rely on IC engines [20].

Only battery electric vehicles (BEV) eliminate the need for IC engines, following the current interest in the electrification of the transport sector. However, life-cycle analyses from well-to-wheel of the GHG emissions of BEVs, that consider the energy used in electricity generation and battery manufacture, show that the reductions in total emissions is much less significant than expected, mainly because of the large lithium-ion batteries [22].

The high cost of electrification is also driving the development of effective, but previously deemed uneconomical technologies to reduce pollutant emission with advanced combustion modes and alternative fuels [20].

Recent development in alternative fuels used in compression-ignition ICEs, the engine type most employed in the marine sector, are namely, hydrogen, ammonia and methanol. All three alternatives are studied for compression-ignition and dual-fuel engines. In the case of ammonia, the slow speed of the flamefront renders it usable only in compression-ignition engines. Methanol is a potent enough to partially replace fossil fuels, however it does not reduce emissions of NO_x and CO, like H₂ and NH₃ [23].

It is true that the mentioned alternative fuels production is in itself a GHG emission activity, since they are obtained from fossil fuels. So, the main goal is actually not reached. However, these fuels can be obtained from electricity from clean renewable energy sources, reducing the overall CO₂ footprint [17].

Biofuels are also an alternative, they represent one of the main solutions to quickly reduce emissions. In Spain, 10% of the main energy company fuel is of renewable origin. The emissions released using these fuels is equal to those that has been previously avoided by employing the raw material for the biofuel production [24].

2.2 Ammonia.

The research on ammonia for internal combustion engines is premature. Only a few research groups have worked extensively on the topic. However, the topic of ammonia as a fuel gained interest recently because of its carbon-free structure, broad availability and easy to handle properties.

2.2.1 Ammonia as an energy vector.

Ammonia has emerged as a promising hydrogen carrier due to its high hydrogen content and relatively simple storage requirements. Unlike hydrogen, which requires extremely low temperatures or high pressures, ammonia can be stored as a liquid under much more moderate conditions. This simplifies logistics, making ammonia a more practical and economical option for mobile energy applications [25][26].

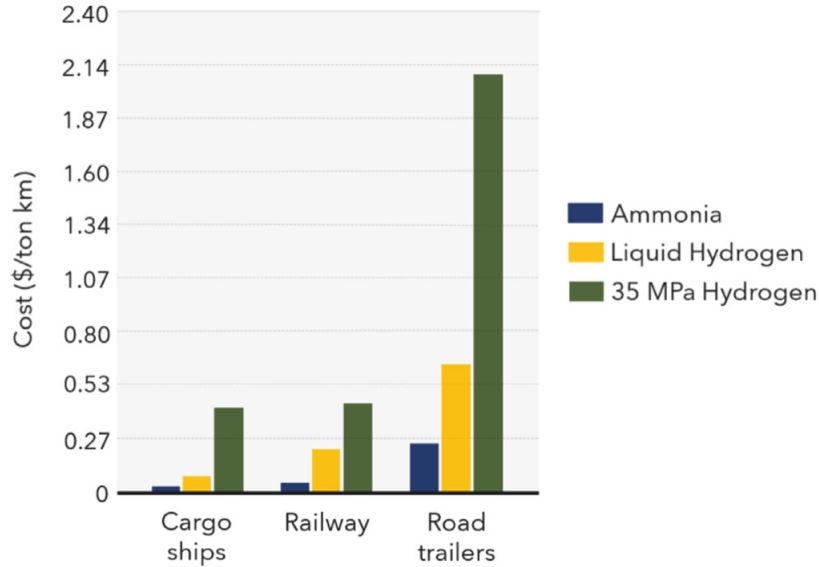


Figure 2.1: Cost estimate for ammonia and hydrogen transportation by principal modes of transport [27].

The ability to decompose ammonia into hydrogen on-site through catalytic processes further enhances its appeal. Ammonia contains 17.6% hydrogen by weight and can be decomposed using metal catalysts [25][26]. This catalytic decomposition allows for the production of hydrogen where and when it is needed, facilitating the adoption of hydrogen in energy systems without the infrastructure challenges posed by direct hydrogen storage.

Ammonia's potential as a hydrogen carrier aligns with the broader vision of supporting the next generation of energy infrastructure based on hydrogen. It offers a safer, less reactive, and more cost-effective means of hydrogen transportation compared to direct hydrogen handling [28]. In addition to its role as a hydrogen carrier, ammonia is also gaining attention as a direct fuel for ICEs. The high energy density of ammonia, approximately 22.5 MJ/kg, is competitive with traditional fossil fuels, making it a viable alternative for powering engines [28].

The use of ammonia as a fuel in ICEs presents several advantages. Firstly, ammonia is a carbon-free fuel, this is important in the context of reducing GHG emissions from the transportation sector. Secondly, ammonia's well established production and distribution infrastructure, provides a ready-made network for its adoption as a fuel [28][26].

On the other hand, there are several drawbacks to using ammonia as a fuel. Its toxicity poses significant safety risks, requiring careful handling measures. Additionally, ammonia has a lower energy density and low heating value (LHV) compared to conventional fuels like diesel, which can limit its efficiency and performance in engines. The slower flame velocity of ammonia also presents challenges for combustion stability and efficiency, necessitating advanced engine optimization to achieve acceptable performance levels. Moreover, ammonia's corrosive nature can lead to material compatibility issues, requiring specialized materials in engine components to prevent degradation.

In conclusion, ammonia's dual role as a hydrogen carrier and ICE fuel highlights its versatility and potential as a foundation of future energy systems. Its storage benefits and environmental advantages can significantly aid in decarbonising the energy and transportation sectors.

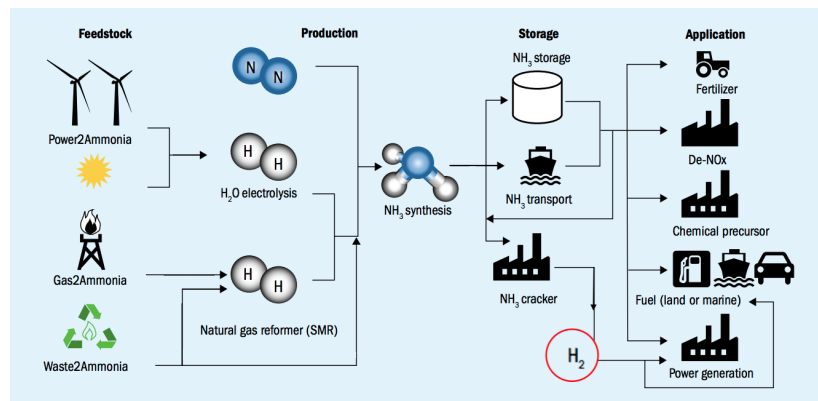


Figure 2.2: Ammonia production and use cycle. (Adapted from [29])

2.2.2 Properties of ammonia.

Ammonia (NH_3) in its pure form is known as anhydrous NH_3 , which is a colourless gas at ambient temperature, with a pungent smell that makes it easily detectable in the air in the range of very few parts per million (ppm), from 0.04 to 53 ppm, being the average 17 ppm. This property comes handy, since ammonia is an extremely toxic molecule if inhaled in big quantities (300 ppm). EU limits are 20 ppm for 8 hours exposure, and 50 ppm for 15 minutes exposure [30][25].

Gaseous NH_3 is much lighter than air, when released in the atmosphere it dissipates rapidly. In the liquid form, its density is approximately 60% of the density of water at room temperature. This, combined with the high solubility in water, makes it easily manageable in case of a spillage [25].

Ammonia is corrosive to materials like copper and its alloys, zinc and it also causes stress corrosion in carbon manganese and nickel steels. Care must be taken when purging air from the systems, ammonia is also reactive with CO_2 that might be contained in inert gases, that is why N_2 is the gas preferred for purging and pressurizing the installations.

The fire and explosion risks are negligible when compared with hydrogen or methane. Needing 2500 and 35000 times more energy to ignite ammonia compared with CH_4 and H_2 respectively [30].

Properties	Units	NH_3	H_2	CH_4	Diesel	LPG
Storage method	-	Compressed liquid	Compressed liquid	Compressed liquid	Liquid	Compressed liquid
Storage temperature	K	298	20	298	298	298
Storage pressure	kPa	1030	102	25	101	1750
Boiling point	K	240	21	112	430	230
Autoignition temperature	K	651	520	630	254	480
Flammability limits (gas in air)	(Vol. %)	16 - 25	4 - 75	5 - 15	0.6 - 7.5	1.8 - 9.5
Low heating value (LHV)	MJ/Kg	18.8	120	50	45	46
Fuel density (at the storage temp.)	Kg/m ³	602.8	71.1	187.2	838.8	0.530
Energy density	MJ/m ³	15.6	120-140	55	45	26
Cetane number	-	0	5 - 10	-	40	-
Octane number	-	110	>130	107	-	110

Table 2.1: Fuel properties comparison. Compiled from [31]&[32]

At standard atmospheric conditions, it is gaseous but can be stored as a liquid by cooling it to -33°C at ambient pressure or without cooling at 10 bar.[17] The viscosity of NH_3 is relatively low and this is potentially beneficial for the fuel atomization and droplet formation during high pressure fuel injection [25].

Although the energy density of stored ammonia is comparably less than gasoline and diesel, it exhibits much higher energy density than compressed natural gas and gaseous or liquid hydrogen. In addition to that, it has a higher octane number than gasoline and natural gas, which allows efficient engine operation at higher compression ratios (CR) [33].

In table 2.1 we can see a comparison of the properties of ammonia and the most common fuels in the marine sector, and hydrogen, the competitor alternative fuel to ammonia.

2.2.3 Emissions.

Ammonia engines suffer from un-burned ammonia and NO_x formation, due to fuel-bounded nitrogen. The formation of N₂O can be produced by two pathways, the first one is due to low temperature of the flame, while the second only happens at higher temperatures. In the latter case, the N₂O usually gets consumed by reacting with atomic hydrogen or by thermal dissociation [34].

Due to incomplete combustion, NH₃ will be discharged in the exhaust. In the case where both ammonia and NO_x are present in the exhaust, it is possible to reduce both simultaneously by using a selective catalytic reduction (SCR) device. Using ammonia as an engine fuel makes the use of SCR attractive since ammonia is already on board of the vehicle [25].

The SCR reaction is as follows [35]:

- $4 \text{NH}_3 + 4 \text{NO} + \text{O}_2 \longrightarrow 4 \text{N}_2 + 6 \text{H}_2\text{O}$
- $8 \text{NH}_3 + 6 \text{NO}_2 \longrightarrow 7 \text{N}_2 + 12 \text{H}_2\text{O}$

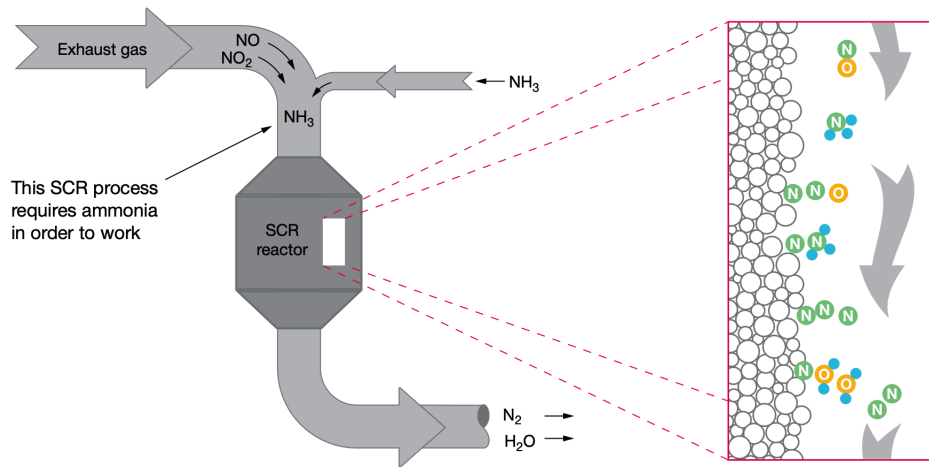


Figure 2.3: Selective catalytic reduction process. [35]

The SCR process shown in figure 2.3 requires equipment that is only feasible for marine or electricity generation applications due to the space demanded for the installation [35].

In the realm of dual-fuel combustion, ammonia has demonstrated reduction in CO₂ emissions when mixed with gasoline or hydrogen in spark ignition engines.

As aforementioned, due to the high auto-ignition temperature of NH₃, the candidate fuel for blending in compression ignition setting must have a high cetane number to improve ignition characteristics, diesel or liquified petroleum gas (LPG) are the targeted fuels in the literature [31][33][35]. In this way, CO and hydrocarbons(HC) emissions reduction has been observed. However, the NO_x emissions variation is inversely proportional to the quantity of NH₃ blended in the fuel [31].

Recently, it has also been proved that NH₃ could inhibit soot formation through chemical mechanisms, in addition to lowering the amount of carbon in the fuel, when blended with diesel-like fuels [34].

Ammonia's production is energy intensive (uses about 2% of the total energy consumed in the world) and it produces approximately 1% of the CO₂ emissions worldwide. In general, the production of one molecule of NH₃ results in the emission of a molecule of CO₂ [36]. That is why efforts to produce green ammonia from renewable energy sources are as important as the ammonia engine development in itself.

2.2.4 Hazards of storage and manipulation of ammonia.

Ammonia is a global commodity that is handled on volumes between 25 and 30 million tonnes annually [37]. There is a large network of ports, pipelines, and dedicated storage facilities and regulations on how to properly handle this hazardous substance. However, using ammonia as a fuel would mean an increase in the human interactions with it, and the overall operations.

The main risk in ammonia operation is leaking. Ammonia is usually stored in liquid form, this implies that the liquid is pressurized or cooled under -33°C at ambient temperature. In case of a leak, the storage conditions will no longer be maintained, and it will change to gaseous phase. The pungent odor of the vapour makes the leak easily detectable. In any way, regulations, protective equipment, bunkering procedures and safe discharge of air or water contaminated with ammonia would have to be developed to reduce the risks and avoid accidents like the 2013 Texas fertilizer plant explosion, linked to improper ammonia storage [38].

Tanks and piping materials must be copper and zinc free, ammonia can easily corrode these metals. Other risk to consider is the pressurization system, when designing it is important to address the specific modes of failure and risks of the installation under extreme conditions.

Purging the systems is also a weak point, nitrogen must be available for purging after operations, for ammonia freeing before, and tightness checking after maintenance. Due to its toxicity, no ammonia should be released to air nor sea as result of normal operations or maintenance. The re-circulation systems have to be redundant and guarantee the severance of ammonia from oils and other substances in the system.

It has been found that most accidents on board of vessels transporting ammonia occur during maintenance of the system [30]. Crews have to be formed to correctly perform maintenance and assess and understand the risks of every operation.

The risks of using ammonia as fuel are comparable to the risk of using other marine fuels such as LPG [39]. Additionally, facilities for handling and transporting LPG are often used for transporting ammonia [40].

2.2.5 Alignment with the SDGs.

The use of ammonia as a fuel is a feasible short-term solution to achieve the Sustainable Development Goals. This section enumerates a correspondance list of the SDGs that fall under the scope of this project to the specific properties of ammonia that tackle them.

SDG 7: Affordable and Clean Energy. Ammonia offers a promising solution for affordable and clean energy. It can be synthesised using renewable energy sources. The fertiliser and chemical industry have created a global infrastructure, with well established standards for the handling and storage of ammonia. Additionally, ammonia can be used as an energy carrier as well as a fuel in ICEs, offering a carbon free alternative to fossil fuels for the transportation and power generation industries [27][41].

SDG 13: Climate Action. The energy contained in green ammonia can be 100% emissions-free if the sources used to make it are supplied from renewable electricity instead of fossil fuels. This potential reduction in GHG emissions is significant, as current ammonia production contributes to high levels of CO₂ emissions. Transitioning to green ammonia, produced via water electrolysis powered by renewable energy, drastically reduces the carbon footprint. Moreover, using ammonia as a fuel for maritime and other transportation sectors can further decarbonise these industries, supporting global climate action goals [29][42].

SDG 14: Life Below Water. Ammonia's role in reducing marine pollution is critical. The maritime industry is a significant contributor to marine pollution, including oil spills and sulfur oxide emissions from traditional marine fuels. Green ammonia, as a maritime fuel, presents an opportunity to mitigate these impacts. Furthermore, the production and use of ammonia align with the objectives of protecting coastal and marine ecosystems by reducing the environmental footprint of the shipping industry [41].

In conclusion, ammonia as a fuel aligns with several Sustainable Development Goals, offering a clean, efficient, and sustainable energy solution. Its adoption not only supports affordable and clean energy and climate action but also contributes to the protection of marine life by promoting cleaner maritime practices.

2.3 Research and state of the art technology on NH₃ fuelled ICEs.

Ammonia fuelled internal combustion engines represent a promising opportunity for reducing GHG emissions. Some projects are leading the way by developing cutting-edge technology and leveraging expertise to address the challenges of using ammonia as fuel.

These are some of the projects that are on the forefront of the research:

DIGIAMMONIA Project

The DIGIAMMONIA project focuses on developing digital technologies to enhance the performance and reduce emissions of ammonia-fuelled engines. Key partners include Universitat Politècnica de València (UPV), with its CMT institute excelling in fluid dynamics and advanced combustion systems. Additionally, the University of Vaasa specialises in ammonia combustion and emission reduction, while Lund University contributes expertise in computational fluid dynamics and engine modelling.

MariNH3 Project

MariNH3, funded by the Engineering and Physical Sciences Research Council (EPSRC), aims to decarbonise the maritime sector through ammonia-fuelled engine technologies. The University of Nottingham leads the research on ammonia combustion in internal combustion engines. Industry partners such as MAHLE Powertrain Ltd and Rolls-Royce Plc are also involved. The University of Nottingham's Powertrain Research Centre has adapted engine test rigs for ammonia research, achieving significant milestones in both compression ignition and spark ignition engines [43].

ENGIMMONIA Project

ENGIMMONIA aims to integrate ammonia-fuelled engines into marine applications, focusing on enhancing engine performance and reducing emissions. The National Technical University of Athens and the Technical University of Munich (TUM) coordinate the project and conduct research on ammonia combustion. While MAN Energy Solutions develops large-scale ammonia engines for marine use, DNV GL ensures compliance with safety and regulatory standards [44].

In a similar vein, MAN Energy Solutions (MAN ES), in partnership with Maersk, has established the Maersk Mc-Kinney Moller Center for Zero Carbon Shipping. This independent research center serves as a collaboration hub for the marine sector, government bodies, and academic institutions [35].

MAN ES is currently developing an ammonia two-stroke ICE engine, which is due for installation on the first vessel by the end of 2024 [35]. Meanwhile, Wärtsilä is concentrating on the development of a four-stroke ammonia ICE engine [45]. In the first quarter of 2024, Wärtsilä secured bookings to deliver the fuel supply system for two new gas carriers, set to operate with ammonia fuel for EXMAR LPG starting in 2025 [46].

Furthermore, there are joint initiatives involving MAN ES, Wärtsilä, DNV, ABB, and major shipping companies to advance engine development and conduct comprehensive analyses of the entire ammonia supply chain and its utilization as fuel [47].

2.4 Regulations.

The marine sector is undergoing major regulatory changes to cut emissions and promote the use of alternative fuels like ammonia. The International Maritime Organization (IMO) aims to reduce greenhouse gas (GHG) emissions by at least 50% by 2050 compared to 2008 levels, and to cut CO₂ emissions per transport work by at least 40% by 2030. These regulations are pushing the maritime industry towards cleaner fuels and new technologies.

Ammonia as a marine fuel is a promising solution for meeting these emission reduction goals. Unlike traditional marine fuels, ammonia does not produce CO₂ during combustion. However, using ammonia comes with challenges, especially regarding nitrogen oxides (NO_x) emissions, which need to be managed through advanced engine technologies and after-treatment systems.

Several international and regional regulations control emissions in the maritime sector. The IMO's MARPOL Annex VI sets limits on NO_x emissions from ship exhausts and bans deliberate emissions of ozone-depleting substances [48]. Emission Control Areas (ECAs) have stricter limits, requiring ships in these areas to meet stringent emission standards.

The European Union has also implemented strict regulations through the European Green Deal, aiming for climate neutrality by 2050. The FuelEU Maritime initiative [49] aims to boost the use of sustainable alternative fuels and technologies by setting greenhouse gas intensity targets for shipping companies.

To comply with these regulations, the maritime industry is exploring various technologies, including the use of ammonia as fuel. These technologies could offer high efficiency and low emissions but need more research and development to overcome technical and economic challenges.

In conclusion, the regulatory landscape is pushing the maritime sector to adopt cleaner fuels like ammonia. Following IMO and EU regulations is crucial for reducing emissions and fighting climate change [42].

2.5 Fuel injection system.

Two of the most commonly used injection systems are the common rail system and the unit injector system. This project focuses on the common rail system, as it is the standard in the industry thanks to its greater flexibility.

2.5.1 Common rail direct injection.

The common rail system gets its name from its main component, the volume of fuel located between the high-pressure pump and the injectors. This volume acts as an accumulator, and also dampens pressure oscillations caused by fuel discharge through the nozzles and the nature of the pump that pressurizes the system.

The operation of the system is quite straightforward. A low-pressure pump takes fuel from the tank and supplies it to the high-pressure pump. The high-pressure pump, driven by the engine crankshaft, pressurizes the fuel in the common rail. The injectors are fed from the common rail, thereby all injectors reach target injection pressure uniformly. The pressure in the rail is regulated by a pressure regulator controlled by the engine's Electronic Control Unit (ECU). If the value measured by the pressure sensors in the rail is higher than the target pressure value, the regulation valve discharges fuel back to the tank until both values are equal.

The disadvantage of this system is the added complexity of having to manage two pumps, as well as increased sensitivity to fuel quality. This is due to the need of more filters and the creation of spaces where fuel impurities could settle, reducing the efficiency of the system in the long term if not maintained properly [50].

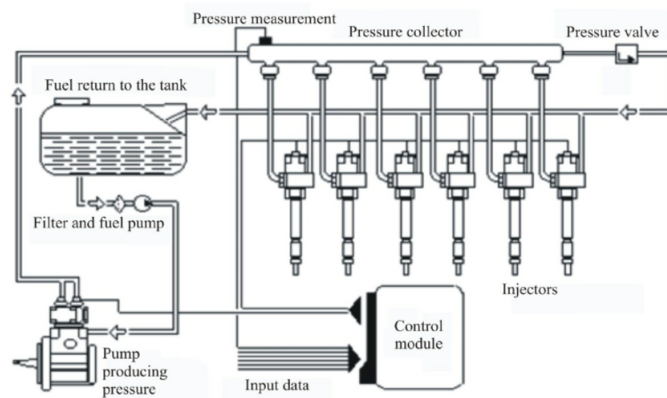


Figure 2.4: Common rail injection system diagram [50].

2.5.2 The injector.

The most complex part of the common rail system is the injector. The injector is controlled by the ECU, which coordinates and defines the injection duration, the rail pressure, and the discharge capacity of the nozzle orifices, thus regulating the amount of fuel injected.

There are two types of injectors based on the internal actuation system: solenoid valve injectors and piezoelectric injectors. The latter are next-generation and not yet widely used. In this project, a solenoid valve injector is employed [50].

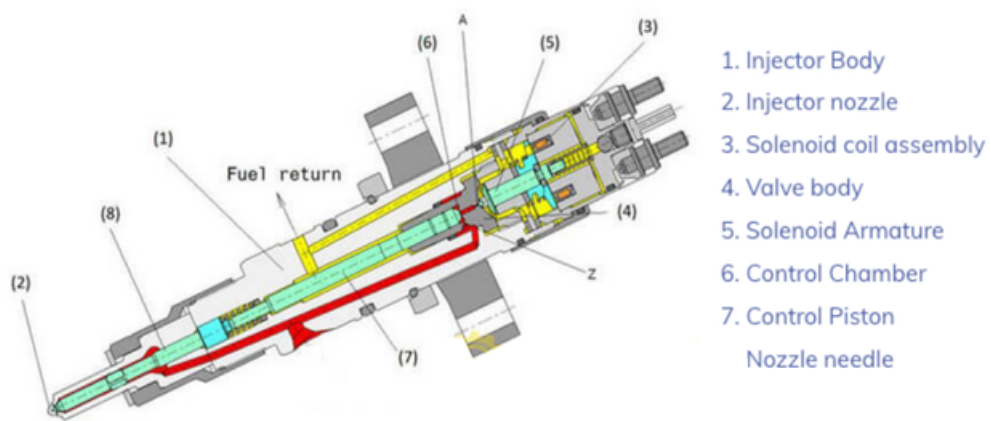


Figure 2.5: Diesel injector diagram [51].

Figure 2.5 shows a generic diagram of a common rail system injector. The injector consists of [18]:

- A nozzle with a spring pressing the nozzle needle against its seat.
- A rod that moves together with the nozzle needle during the injection process.
- An orifice that supplies fuel to a control volume where the top of the rod is located.
- An orifice for the control volume's exit, whose opening and closing are controlled by a solenoid valve.

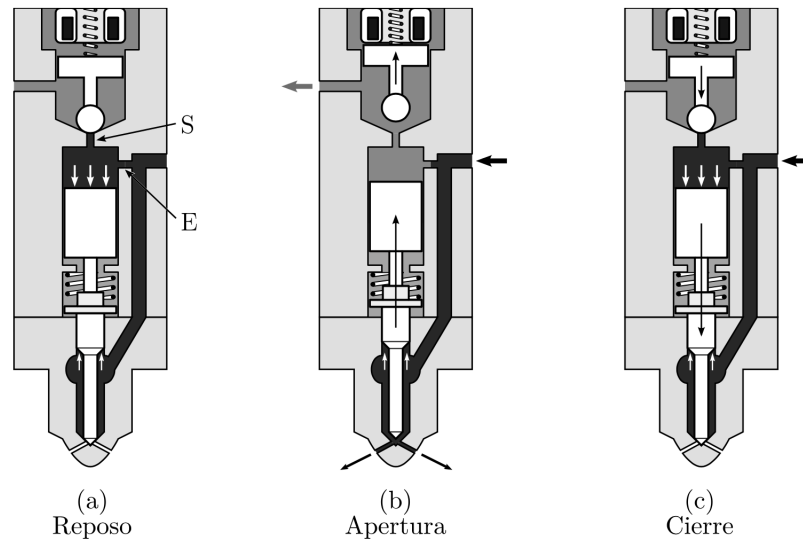


Figure 2.6: Operation of a common rail injector [18].

The pressurized fuel from the common rail is divided into two streams: the primary flow is injected into the cylinder, while the secondary flow is used to control the injector.

When the solenoid is deactivated, the orifice S is closed (fig 2.6a). The fuel pressure, equal to that of the common rail, acts on the top of the rod through orifice E and on the bottom of the nozzle needle.

Since the upper section of the rod is larger than the lower section of the needle, along with the pretension force of the spring, the needle remains seated, and the nozzle orifices are closed.

Once the solenoid is activated, orifice S opens, reducing the pressure in the control volume (figure 2.6b). In this situation, the pressure on the top of the rod is lower than on the bottom of the needle, causing the rod-needle assembly to lift, uncovering the nozzle discharge orifices and generating injection.

The control flow released through orifice S returns to the fuel tank. When the solenoid valve is deactivated again (figure 2.6c), orifice S closes, the pressure on the top of the rod is restored, causing the rod-needle assembly to descend, closing the nozzle orifices, and ending the injection [18][50].

2.5.3 How much may ammonia differ from diesel in injection.

While there is extensive literature regarding the behaviour of conventional diesel-like fuels sprays under direct-injection high-pressure conditions, research on ammonia is limited.

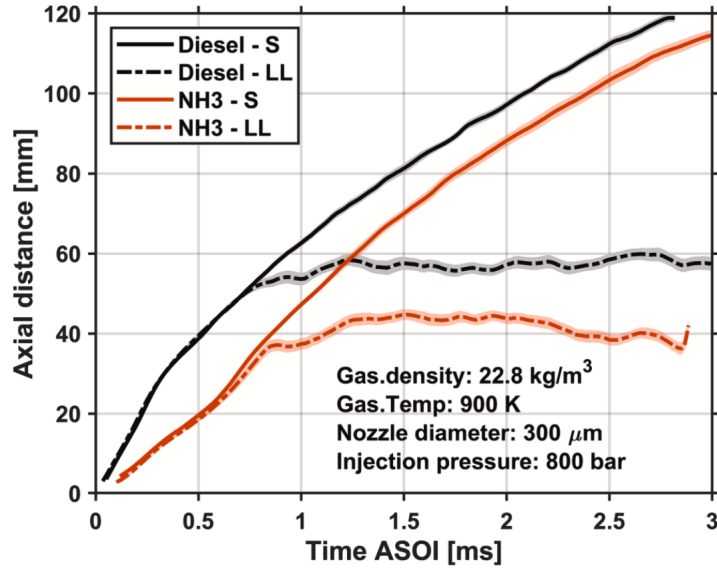


Figure 2.7: Vapor and liquid spray penetration evolution for diesel and ammonia [52].

Recently, Payri et al [52] performed measurements of the spray using ammonia in engine-like conditions (in terms of chamber pressure and temperature), then compared the results with conventional diesel fuel. They have noticed differences in the spray development.

Observing figure 2.7, both fuels show a linear trend of penetration over time. However, ammonia is noticeably slower, suggesting a lower momentum flux within the spray. This phenomenon may be attributable to the internal flow dynamics of the injector during ammonia injection. Specifically, the different viscosity of ammonia likely induces significant frictional losses within the injector sac, thereby slowing down the injector needle.

There is a scarcity of references in the literature regarding the hydraulic characterization of ammonia injection. This gap in knowledge motivates this project.

Directly measuring the momentum flux of both diesel and ammonia will help in the understanding of the observed difference in spray dynamics. This data will shed light on the reasons behind the slower penetration of ammonia and contribute valuable insights to the ongoing research.

2.6 Momentum flux. Definition, utility and experimental measurement technique.

Studies that approach the effects of different injection strategies usually require complex facilities to measure the injection rate accurately on the engine test bench. This is why it is more common to use experimental procedures to characterise the fuel injection process. Two of the main methods are the rate of injection and the momentum flux.

This project focusses on the momentum flux method. This method is used because, as aforementioned, ammonia's corrosive properties render it incompatible with commercial measurement devices for mass flow rate and hydraulic characterization.

The lineal momentum is defined as the product of mass and velocity. In the context of an injection jet, momentum flux refers to the flow of linear momentum through the exit area of an injector nozzle.

Momentum flux measurement is crucial for understanding various aspects of the injection process in diesel engines. It helps in:

- **Estimating exit velocity.** Provides a more accurate estimation of the exit velocity of the jet compared to mass flow measurements alone.
- **Determining effective flow area.** Helps in calculating the effective flow section at the nozzle exit.
- **Analyzing spray characteristics.** Key parameters like spray penetration, spray angle, and air entrainment depend significantly on momentum flux.
- **Studying internal nozzle flow.** Offers deeper insights into internal flow characteristics, including the effects of nozzle geometry and cavitation phenomena.

The momentum flux rate is defined as:

$$\dot{M} = \int \rho u (u \cdot dA) = \rho u^2 A \quad (2.1)$$

Considering that the mass flow rate can be expressed as:

$$\dot{m} = \int \rho_f u \cdot dA = \rho_f u A \quad (2.2)$$

Both magnitudes can be related by expressing the mass flow rate as a function of the momentum flux rate and the properties of the nozzle and fuel.

$$\dot{m} = \sqrt{A \rho_f \dot{M}} \quad (2.3)$$

Where A is the area of the nozzle, ρ_f is the density of the fuel used, and \dot{M} is the momentum flux rate measured.

In this way, we indirectly measure the mass flow of ammonia.

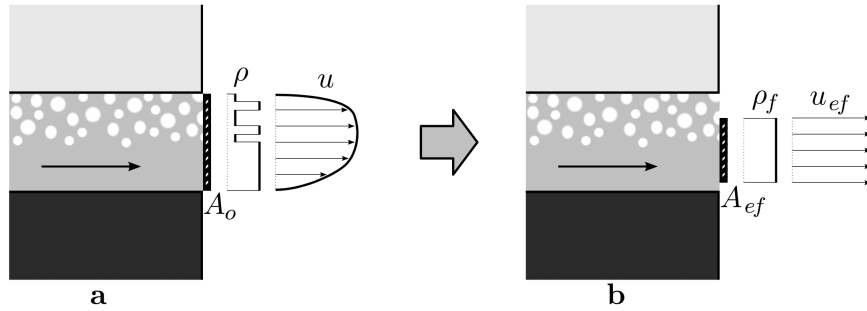


Figure 2.8: Definition of effective area and velocity [18].

However, the flow is not homogeneous across the entire cross-section of the nozzle; nevertheless, it is possible to define effective velocity and area to consider a simplified and representative flow. The equations convert to:

$$\dot{M} = A_{eff} \cdot \rho_f \cdot u_{eff}^2 \quad (2.4)$$

$$\dot{m} = A_{eff} \cdot \rho_f \cdot u_{eff} \quad (2.5)$$

Combining equations 2.4 & 2.5 we can get both the effective area and effective velocity of the nozzle:

$$A_{eff} = \frac{\dot{m}^2}{\rho_f \cdot \dot{M}} \quad (2.6) \quad u_{eff} = \frac{\dot{M}}{\dot{m}} \quad (2.7)$$

Equations 2.4 & 2.5 can also be used to define the discharge coefficient C_d :

$$C_d = \frac{\dot{m}}{A \cdot \rho_f \cdot u} \quad (2.8)$$

Which can be decomposed into two coefficients, C_a for area and C_v for velocity:

$$C_d = C_a \cdot C_v \quad (2.9) \quad C_a = \frac{A_{eff}}{A} \quad (2.10) \quad C_v = \frac{u_{eff}}{u} \quad (2.11)$$

Having these coefficients determined completely characterises the hydraulic behaviour of the injector.

With the momentum flux defined and its usage explained, the next step is to develop the experimental measurement principle used in this project.

The principle of measuring momentum flux relies on the impact force of the spray jet. When the jet impacts on the piezoelectric force sensor, the sensor captures the force exerted by the injection jet. This force corresponds to the momentum flux (\dot{M}) at the orifice exit by the conservation of momentum in the axial direction.

The conservation of momentum in a cylindrical control volume, as shown in figure 2.8, is valid only if the following conditions are met:

- The gravitational forces on the control volume are negligible compared to the other terms,
- The pressure in the chamber is uniform. Consequently, the sum of forces due to pressure is simplified to only the force exerted on the sensor,
- The injector nozzle, and therefore the fuel jet, are perpendicular to the force sensor.

- The direction of the air entering the control volume and the direction of the fuel exiting the collector are perpendicular to the jet axis. This means that the momentum flux through the outer surface will be zero in the axial component.
- It is considered that the system is stationary.

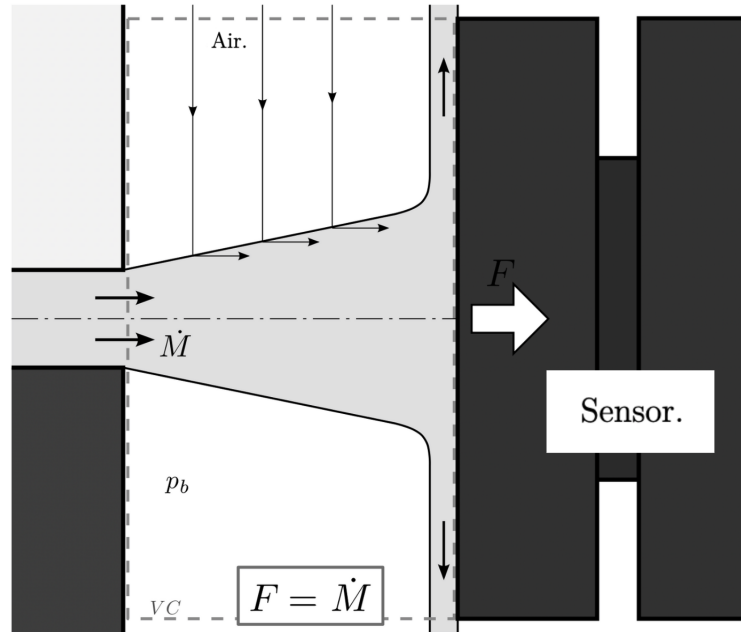


Figure 2.9: Measuring principle of momentum flux. Adapted from [18].

These conditions allow to develop the following considerations, which significantly simplify the measurement process:

The density of the gas used to pressurize the chamber will not affect the measurement of momentum flux, so any gas can be used without impacting the measurement.

Additionally, due to the conservation of momentum in the axial direction, the distance between the force sensor and the nozzle will not affect the measurement, as long as the jet deflects perpendicular to the injection axis.

This method has been validated and used in previous projects, providing reliable results for conventional fuels. the novelty is its implementation for the ammonia injection process characterization [18][53].

Chapter 3

Re-design of the test-rig and set-up of the experimental installation.

In this chapter, the re-design and setup of the test-rig to accommodate ammonia as a fuel is presented. The purpose of this modification is to create an experimental installation capable of handling the properties of ammonia. This chapter is divided into several sections, each detailing the specific aspects of the re-design, from the initial state of the existing test-rig to the modifications made, and the final setup of the experimental installation.

3.1 Starting point.

Available momentum flux test-rig.

The initial step is to evaluate the existing momentum flux test-rig. This section will describe the current setup so we can identify the necessary modifications to adapt the test-rig for ammonia.



Figure 3.1: Front view of available test-rig.

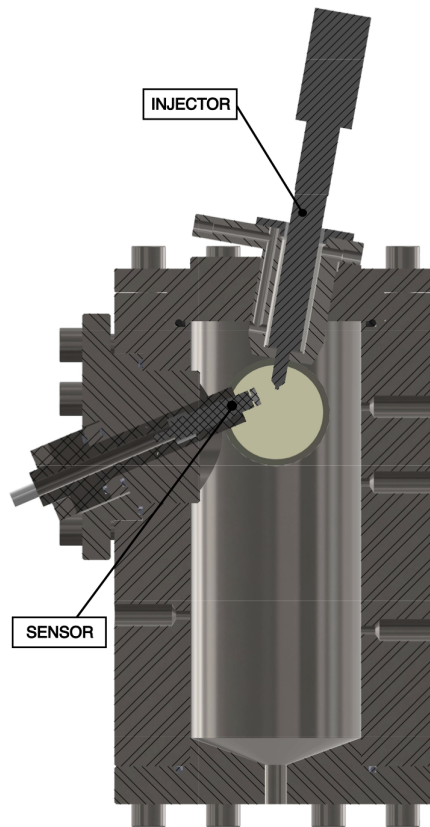


Figure 3.2: Cross section of available test-rig.

The original momentum flux test-rig was designed and developed at the CMT by Jaime Gimeno as part of his mechanical engineering PhD Thesis [18]. Initially conceived for diesel fuel applications, the test-rig has also been used for AdBlue injection research, providing crucial data on injection rates and the hydraulic characterization of various injectors.

The test-rig consists of a stainless steel main vessel with docks to insert the injector and sensors, as well as an opening for visualization of the inner components. This vessel can be pressurized to simulate engine-like conditions when studying injector behavior. The back-pressure (BP) can be regulated up to 100 bar by injecting a pressurized inert gas like nitrogen or helium to avoid combustion hazards.

These high pressures require the vessel to be completely sealed to prevent any leaks to the exterior and between components inside the test-rig, particularly to avoid nitrogen or fuel leakage into the refrigeration system of the injector holder.

To achieve this, a set of gaskets are distributed at every contact surface, and the nuts are tightened to a torque of 25Nm.

In the configuration shown in figures 3.1 & 3.2, the injector and sensor are angled because the used injector had a multiple orifice nozzle. The momentum flux can be measured for only one fuel jet at a time. The injector used to be rotated so each orifice faced the sensor perpendicularly, hence the injector inclination.

The injector holder plays a crucial role by positioning the nozzle at the correct angle and regulating the temperature of the injector body to simulate real injection conditions. The refrigeration system uses glycol to maintain the injector at an operational temperature ranging from 15°C to 70°C.

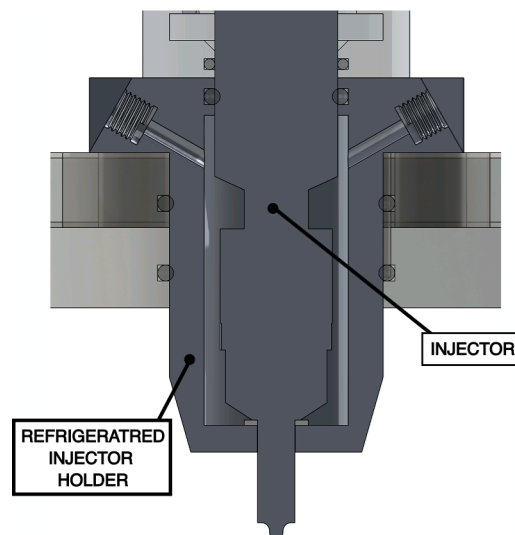


Figure 3.3: Refrigerated injector holder cross section.

Figure 3.3 shows a cross-section of the new injector holder assembly. The working principle of the refrigeration process remains the same as in previous models, in figure 3.2 we can see the previous injector holder. Glycol enters from one side, circulates around the injector body to regulate the temperature, and then exits from the other side.

In figure 3.2, it can be seen a set of orifices on the vessel walls. These orifices are used for placing sensors (thermocouples and pressure gauges) and for pressurization and purging. Additionally, the lower cover has a drain connected to a valve for evacuating the fuel injected during experiments.

3.2 Description and justification of the modifications made to adapt the test-rig to ammonia conditions.

Modifying the test-rig to safely use ammonia involves several changes. This section discusses these modifications, each designed to address the specific properties and handling requirements of ammonia.

3.2.1 Gaskets.

Gaskets are mechanical seals that fill the space between mating surfaces, preventing leaks while under compression. In the original test-rig, Viton gaskets were used, which are made of a type of synthetic rubber and fluoropolymer elastomer. Despite its remarkable characteristics, Viton is not compatible with ammonia due to its corrosive nature, which degrades the rubber. Therefore, we need to replace the gaskets in the test-rig with new ones made from a compatible material.

After comparing various materials, EPDM (Ethylene Propylene Diene Monomer) was chosen since it is a synthetic rubber widely used for gasket manufacturing due to its high chemical resistance and elasticity.

To order the new gaskets, measuring the existing ones when available, and also using the CAD model of the test-rig were the taken approach to get the dimensions.

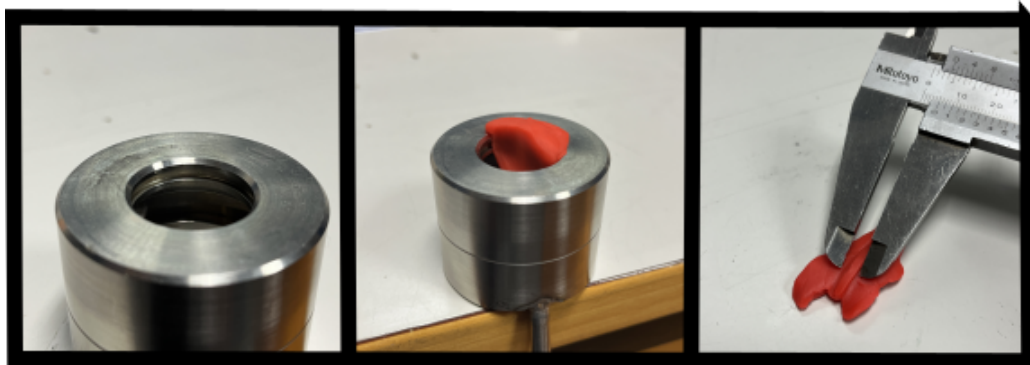


Figure 3.4: Indirect measurement of o-ring groove dimensions.

When no Viton gasket were available and the CAD file was not accurate, indirect measurement methods were resorted to. For instance, to model the injector holder and measure the necessary O-ring, modeling clay was used to create an impression of the groove, see figure 3.4. This impression was then measured with vernier calipers, as direct measurement was not possible due to the limitations of the tools available.

After identifying and measuring all gaskets in the test-rig, the order was made increasing the required quantity to ensure a security stock for spare parts. The list of ordered gaskets is shown in Table 3.1.

ID	d1	d2	Needed Quantity	Ordered Quantity
1	23	1.55	1	8
2	24.6	3	3	8
3	61	2	1	3
4	62	2.5	1	3
5	74	3	1	3
6	95	4	1	12
7	100	3	1	3

All measurements in millimeters (mm).
 "d1" and "d2" referred in figure 3.5.
 Material: EPDM

Table 3.1: Table of ordered o-rings.

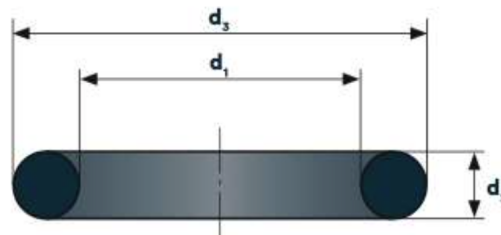


Figure 3.5: O-ring diameters definition.

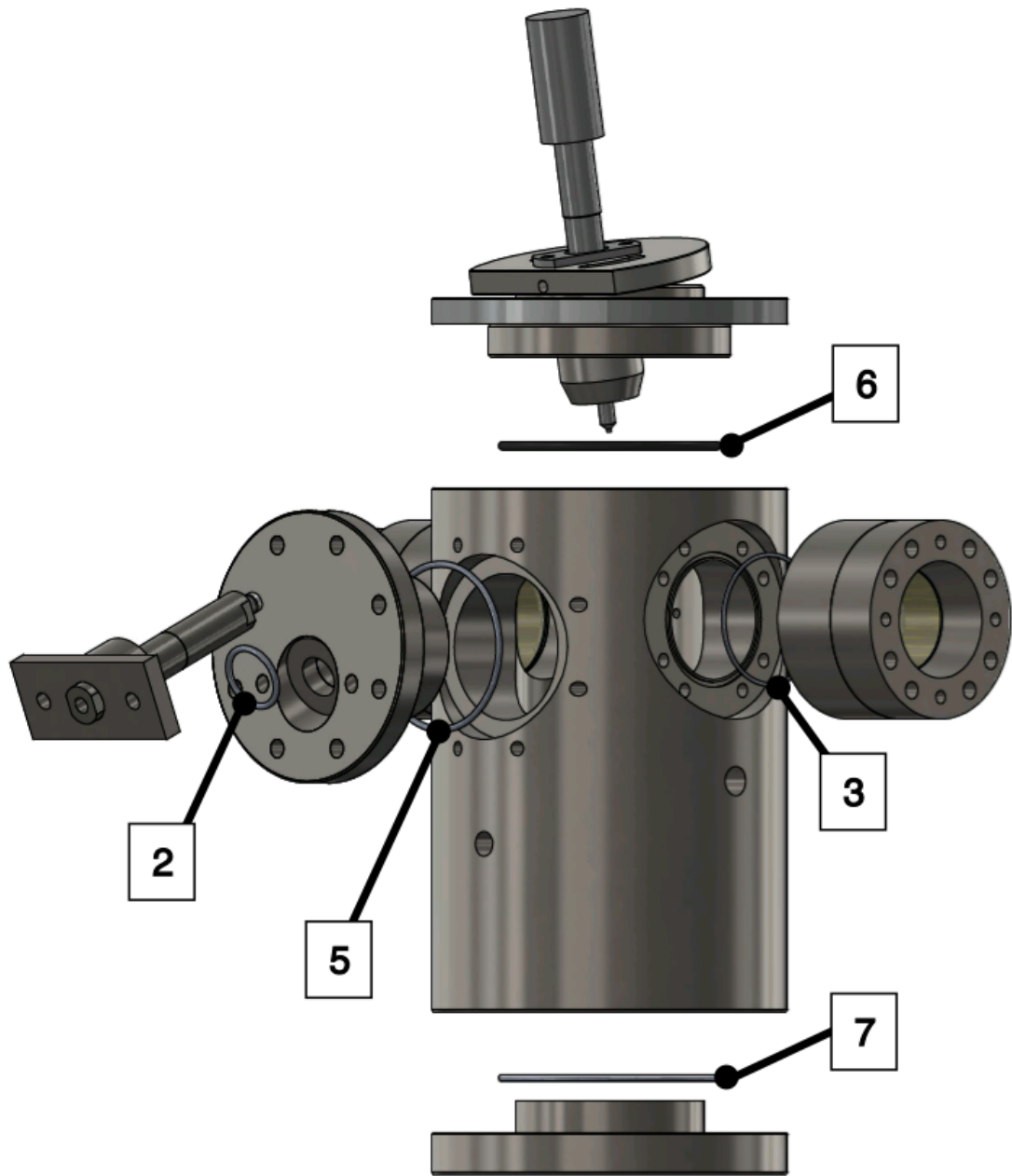


Figure 3.6: Exploded view of gaskets in the test-rig.

Figure 3.6 shows a view of the replaced gaskets. Tags are defined in table 3.1.

Another crucial sealing element is the ring gasket that seals the injector nozzle (see figure 3.7). This ring separates the refrigeration system of the injector holder from the pressurized vessel containing the fuel and nitrogen.

It was originally a copper gasket. Since ammonia corrodes this material, it has been changed to Teflon, which is a synthetic polymer compatible with NH_3 . This gasket is considered disposable because, to ensure a proper seal, the injector must be pressed against it to the point of deformation. The sealing torque applied is 20 Nm, which is the ideal value to ensure proper sealing. If the gasket is over-tightened, it deforms excessively, leading to leaks. Therefore, once the injector is removed or decompressed, the gasket must be replaced to prevent any leaks.

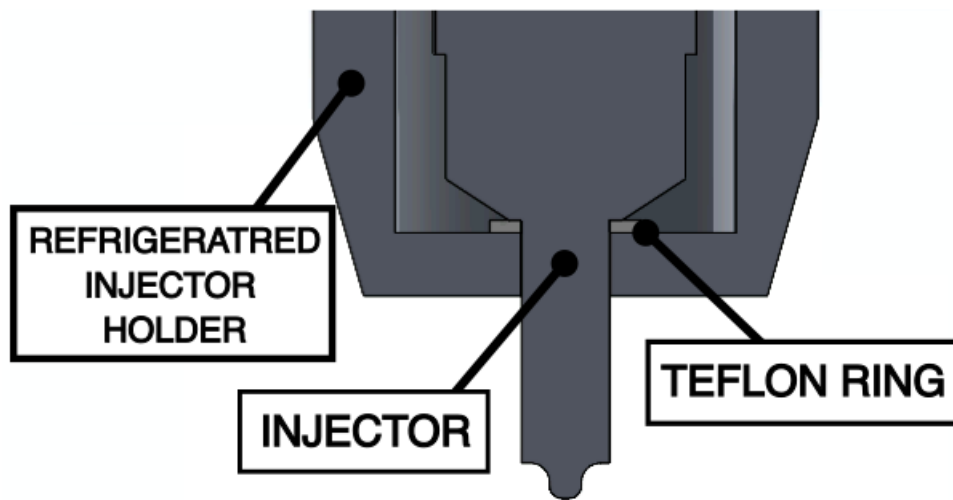


Figure 3.7: Teflon gasket close-up view.

3.2.2 Injector holder.

The injector holder ensures the proper positioning of the injector, as well as maintaining the injector at the desired operation temperature. Originally, the test-rig was designed to accommodate a multi-orifice nozzle injector, which required the injector to be inclined to accurately measure the momentum flux from individual fuel jets. The inclination was necessary because the injector had to align each orifice perpendicularly to the sensor to measure.

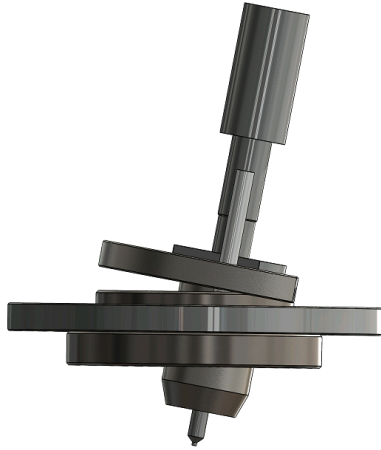


Figure 3.8: Angled injector holder.

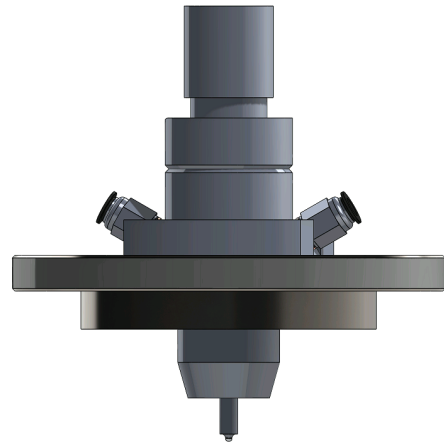


Figure 3.9: Straight injector holder.

The single-orifice Spray D injector for this project is positioned co-axially with the test-rig, eliminating the need for inclination. This change was made because the single orifice allows for direct alignment with the sensor when placing the sensor directly under it, simplifying the positioning of the target. This meant replacing the previous angled holder with a straight one.

The change to ammonia as a fuel required more modifications to the holder. Due to ammonia's physical properties, it requires a larger nozzle diameter than the employed for diesel in the original design to ensure proper injection without clogging or other issues. Consequently, the inner diameter of the new injector holder had to be increased to accommodate the larger injector. The outer diameter is restricted because any modification to this dimension would mean re-designing the top lid of the test-rig, which is unnecessary. These adjustments ensures that the injector holder can securely house the new injector and maintain its functionality.

3.2.3 Sensor holder.

As aforementioned, the original test-rig was equipped with a multi-orifice nozzle, needing the sensor to be positioned at an angle (fig. 3.10). This setup allowed the sensor to be perpendicular to each orifice by rotating the injector, ensuring accurate momentum flux measurements from individual fuel jets.

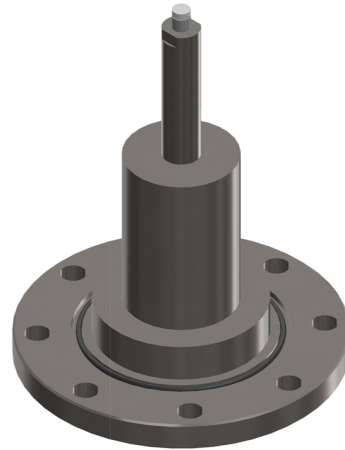
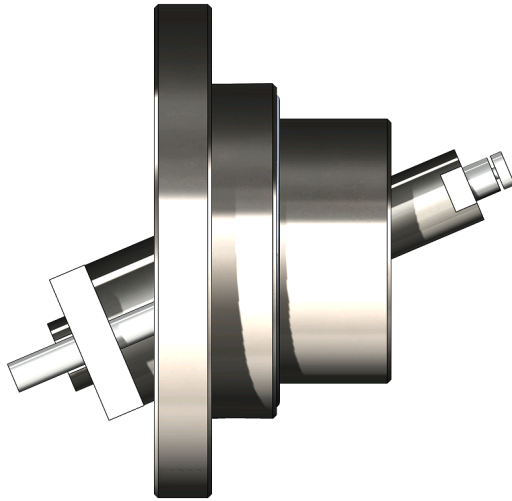


Figure 3.10: Angled sensor holder. **Figure 3.11:** Straight sensor holder.

In the updated configuration, the single-orifice injector is positioned vertically, eliminating the need for the angled sensor (fig. 3.11). Consequently, the sensor holder has been modified. The new sensor holder is straight and introduced from the base of the vessel. This design needs relocating the fuel drain valve to the side of the vessel. The previous sensor holder remains installed to cover the side opening, with the sensor replaced by a metal plug.

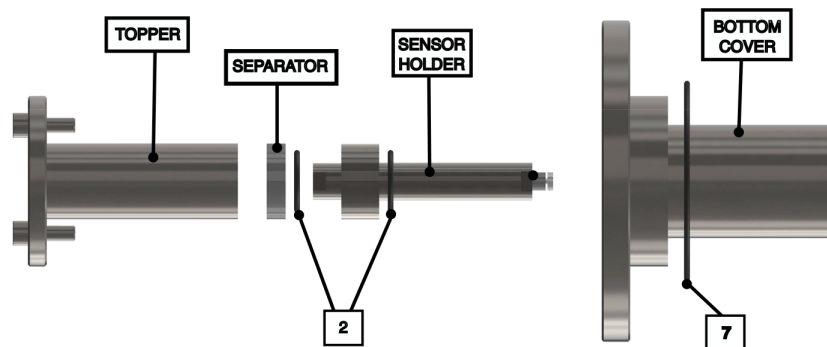


Figure 3.12: Exploded view of sensor holder assembly.

Depending on the length of the injector, the distance between the nozzle and the momentum flux sensor may vary. To adjust this distance a metal separator disc is used. Each separator has a corresponding o-ring to ensure a leak-free connection, as shown in figure 3.12.

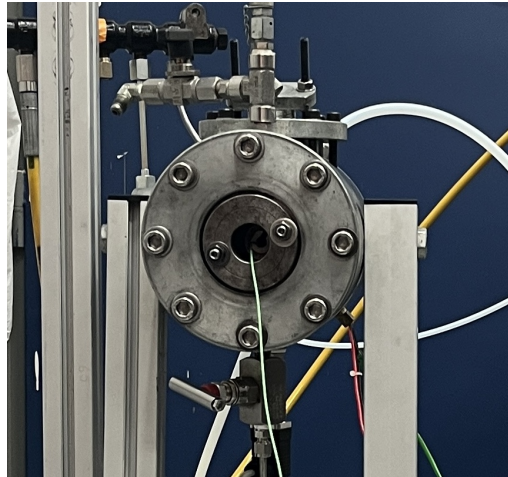


Figure 3.13: Sensor configuration view on the test-rig.

Figure 3.12 represents, from left to right, the topper, with the fixing bolts; separator and o-ring; sensor shell, o-ring and the sensor; and finally the lower cover of the vessel. And in figure 3.13 we can see the actual test-rig assembled.

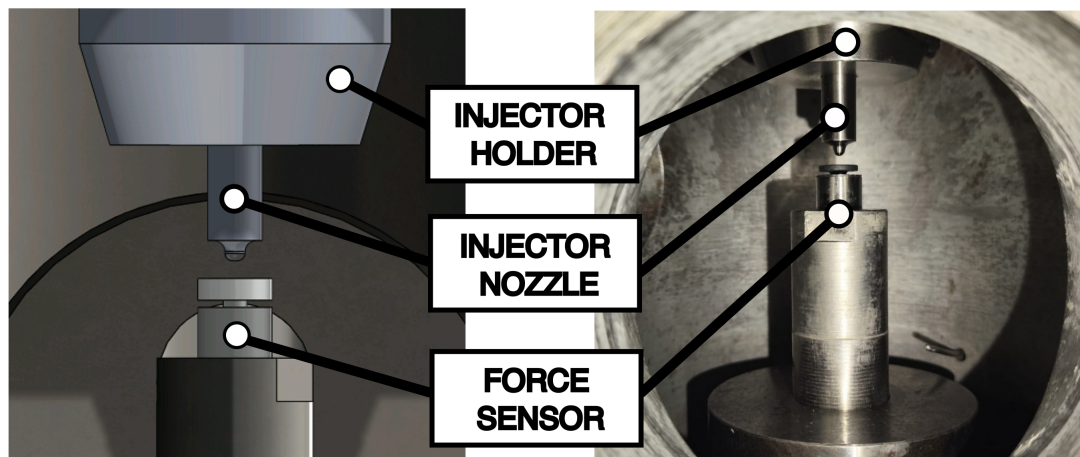


Figure 3.14: Modeled and actual nozzle-sensor view.

Figure 3.14 shows the new sensor disposition, both in the test-rig and the render of the model.

3.2.4 Fuel return collector sleeve.

The injectors of the project expel the control flow through an orifice on the side of the injector body, instead of the top, which is more common. This design requires the use of a fuel collection device named as return sleeve. The return sleeve is a cylindrical component made of stainless steel that fits over the injector, creating a jacket to collect the returned fuel mass flow. The sleeve's design is straightforward. It is a cylinder with a wider internal chamber to collect the fuel, a drain channel, and an o-ring gasket on the bottom diameter.



Figure 3.15: Return sleeve model.

The sleeve is tightly fitted to the injector body and sealed with two o-rings, one on the sleeve and one on the injector.

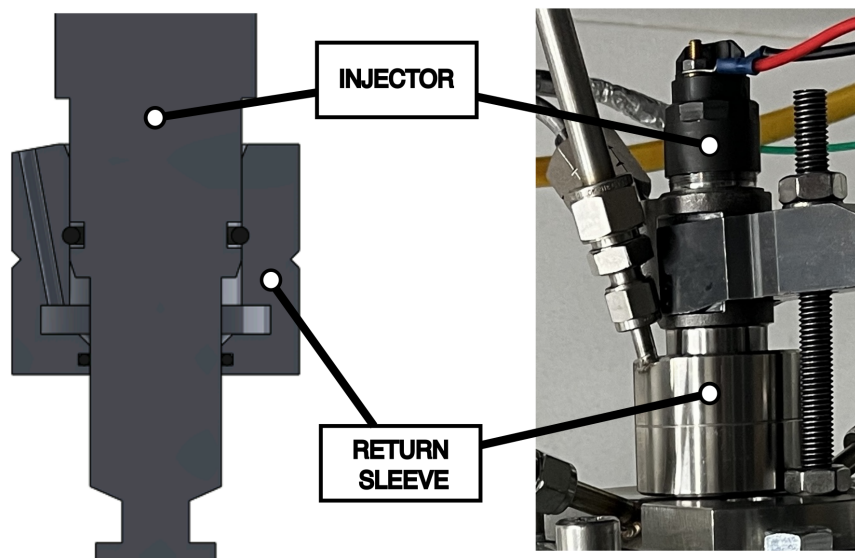


Figure 3.16: Return sleeve model and actual assembly.

3.2.5 Re-designed assembly.

This section presents a render of the final assembly of the modified test-rig.

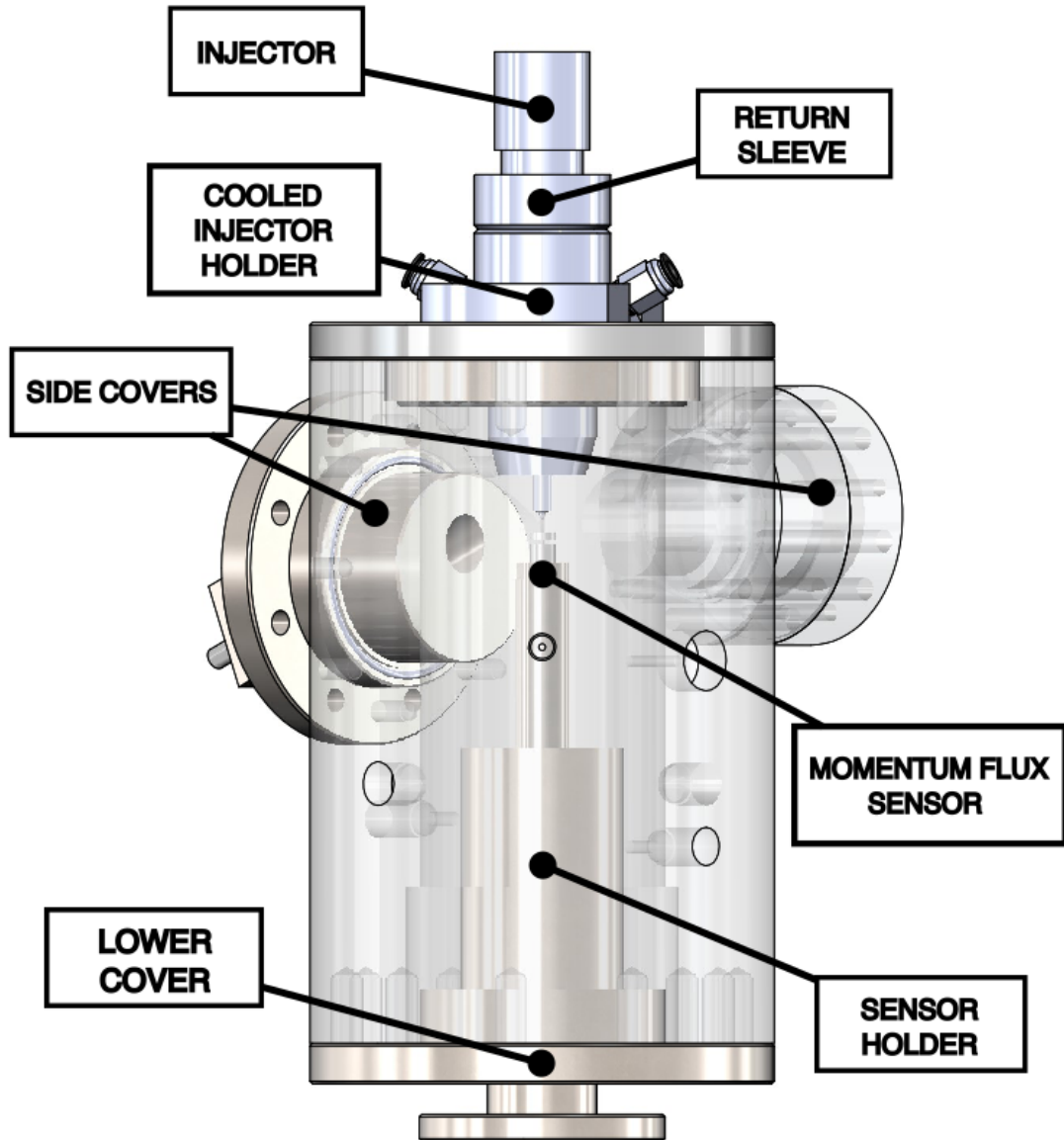


Figure 3.17: Modified test-rig model for ammonia.

3.3 Set-up of the experimental installation.

This section provides an overview of the experimental installation, detailing the components and their role in the system.

3.3.1 Mechanical Installation

The experimental setup consists of several key components essential for its operation. At the core is the test-rig, which serves as the primary site for fuel injection and momentum flux flow measurements.

The test-rig is equipped with a pressure system that uses nitrogen to simulate engine-like conditions by pressurizing to the desired back pressure (BP). This system consists of a nitrogen tank connected to the main vessel via a manometer, which regulates the nitrogen flow into the test-rig to reach the desired BP.

In this project, a single-orifice nozzle injector is used. The injector type corresponds to Spray D from the "Engine Combustion Network" consortium [54]. Two nozzle diameters are being tested, 200 μm and 300 μm . The objective is to determine if commercial injectors can withstand operation with ammonia.



Figure 3.19: Injector.

This type of injector has the back-flow return on the side instead of the top of the body. To address this, a sleeve was designed to create a jacket for fuel collection and discharge. All back-flow, purge, and leakages are routed to a common collector directed to an acid trap, which consists of a large water container situated on the rooftop for safety measures. The entire ammonia circuit is tested to be leak-proof, although the lab is equipped with a ventilation system that must be on during and after the measurements.

A critical component for direct injection is the common rail. In our setup, we are using a heavy-duty common rail capable of withstanding pressures up to 2500

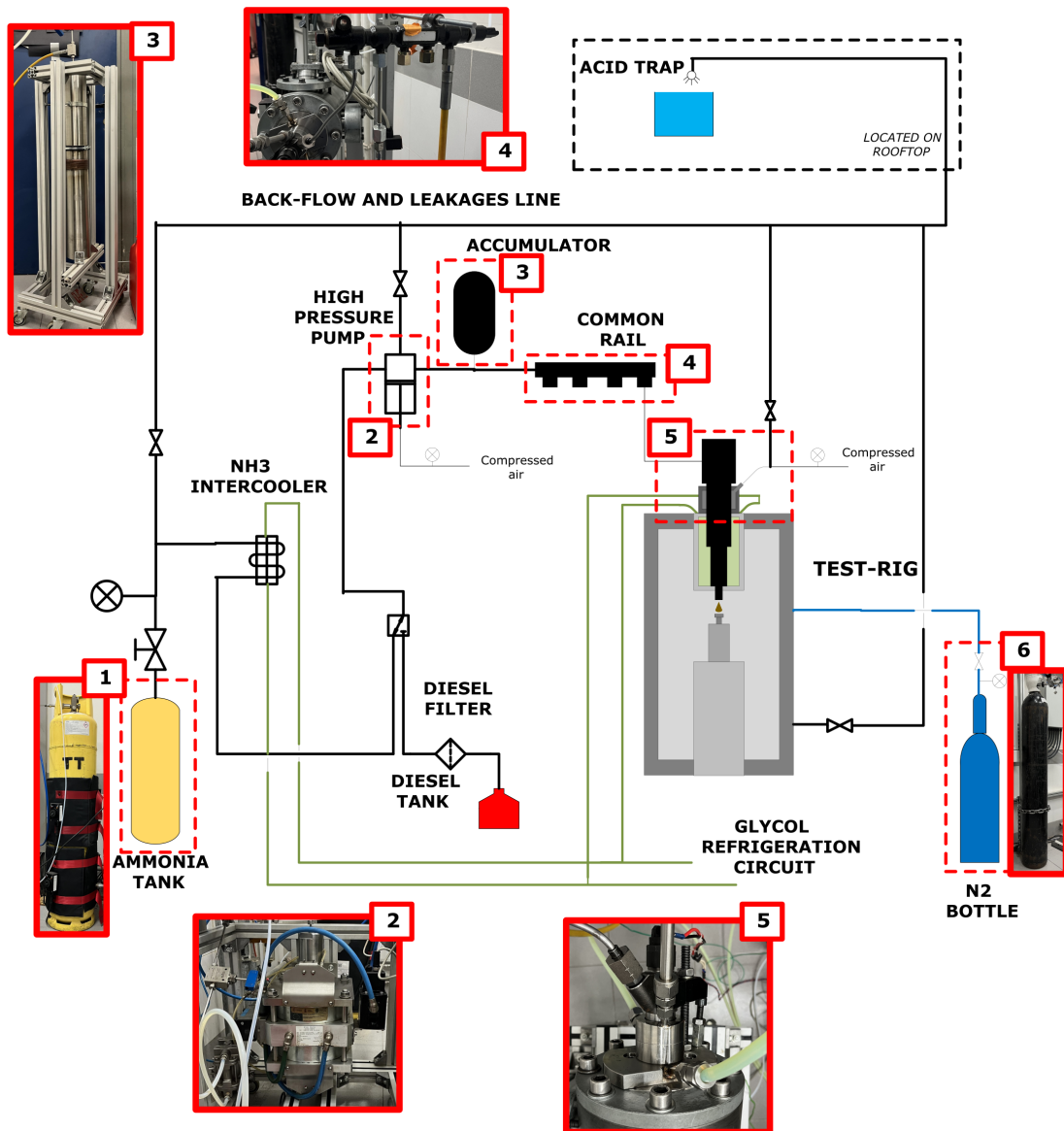


Figure 3.18: Experimental installation diagram.

bar. Additionally, there is an accumulator between the high-pressure pump and the common rail to smooth pressure oscillations that are a consequence of the pneumatic pump operation.

The fuel system is pressurised by a high-pressure pneumatic piston pump. This type of pump was chosen because other alternatives, such as centrifugal pumps, are incompatible with ammonia. Previous experiments at CMT have noticed that

ammonia leaks and deteriorates rotary pumps. The selected pump can reach pressures of up to 4000 bar, however our experiments are conducted in the 400-800 bar range. At low pressures, the pump's PID controller struggles to maintain a constant pressure, hence the need of the accumulator in the common rail system. This pump operates by compressing a piston on one side with compressed air from the building installations, which then moves another, smaller piston with a much greater compression ratio. Fuel is compressed in this second piston. The pressurised air intake of the pump is controlled from the computer.

The fuel supply differs for diesel and ammonia. Diesel is contained in a container at ambient pressure and temperature, and passes through a filter before reaching the high-pressure pump. On the other hand, liquid ammonia is extracted from a high-pressure container and then passes through an inter-cooler before reaching the pump. Refrigeration is crucial to prevent phase changes that cause cavitation.

To ensure that ammonia remains in a liquid state until injection, two solutions were implemented. The injector holder functions as a cooling jacket, keeping the injector body around 15°C. Both the pre-pump ammonia inter-cooler and the injector holder are refrigerated with a closed glycol circuit. To increase the reliability of the results, the injector is cooled even when working with diesel, although it is not necessary for the correct functioning of the injector.

The second solution proposed is pressurising the back-flow and leakages line to 8 bar with compressed air sourced from the pneumatic installation of the CMT. Diesel injection will be tested in both scenarios, with and without the pressurised return line, to have a broader dataset.

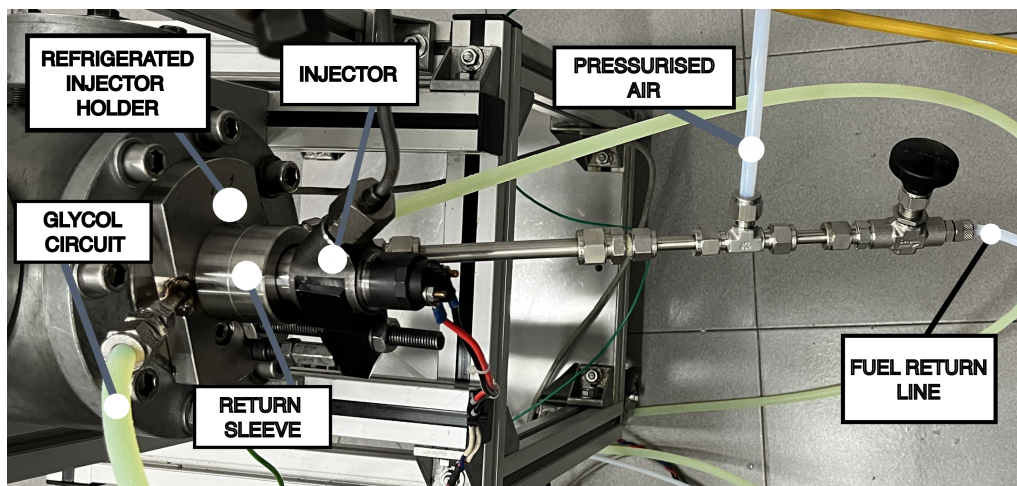


Figure 3.20: Close up view on the refrigeration circuit and the return sleeve.

3.3.2 Electric Installation

This subsection presents the electronic components within the experimental set-up, essential for the control and data acquisition.

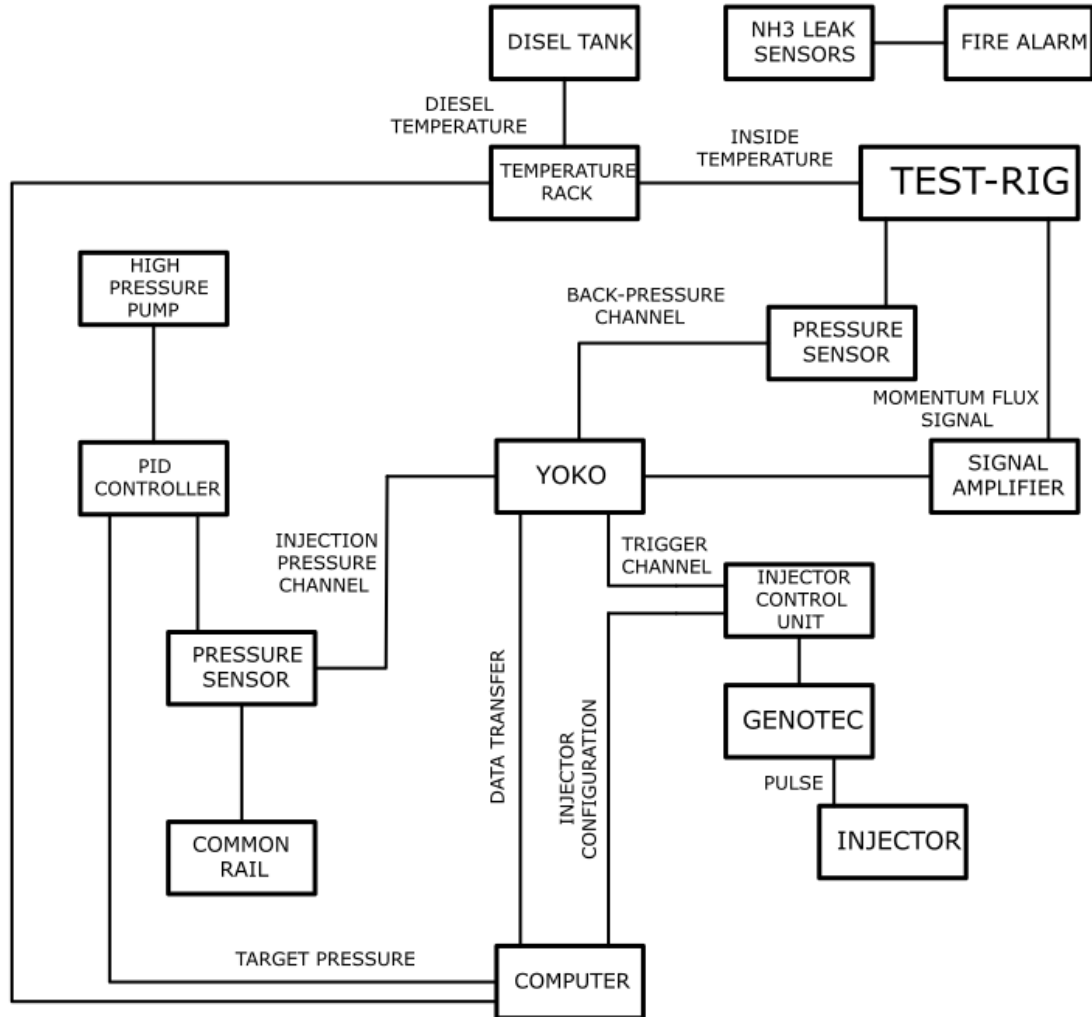


Figure 3.21: Electronic system diagram.

The diagram in figure 3.21 is a representation of the different elements in our installation.

The YOKO (fig. 3.22) is the data acquisition device, data from all sensors are logged in real time, recording to the computer the selected data of measurements. These data points timing correspond with the injector trigger. The injection pulse

parameters and frequency are configured in the PC, however the Injection Control Unit (ICU) is the device in charge of creating the trigger signal and communicating with the GENOTEC, the device that sends the electric pulse to the injector.

The momentum flux is measured with a pressure sensor, piezoelectric sensors are also used for measuring back-pressure values inside the vessel and the injection pressure in the common rail. The latter is both recorded for the experiment and is an input for the high-pressure pump PID, the device that actuates the pump to maintain the pressure in the rail as close as possible to the objective pressure value defined in the PC.

Temperature is controlled with thermocouples situated in points of interest, these sensors are not connected to the YOKO, they are directly connected to the PC.

To ensure safety, ammonia leak detectors are placed both in the experiment room and the adjacent spaces of the CMT, being directly connected to the fire alarm system, to evacuate the facilities in case of an emergency.



Figure 3.22: YOKOGAWA digital scope.

3.4 Experimental installation.



Figure 3.23: Experimental installation.

Chapter 4

Methodology.

In Chapter 2 the theoretical background and measuring principle were explained, and in Chapter 3 the test-rig was presented. This chapter will focus on explaining the actual measurement process and some key considerations, as well as presenting the test plan that will be followed.

4.1 Software employed.

The presented hardware is controlled via the following software, in this section we also present the software employed for the data processing.

Excel worksheet

To ensure correct data processing by the Xtasutiles program, it is necessary to complete the table in Fig. 4.1 during the measurement process.

Nombre Medida	Proyecto	Tobera	Punto	Orificio	Repe	Pinyobj	CPobj	CP	Tmaq	Teb	npulsos	DT1	ET1	Combust	Gas
Digiammonia_300_p01_P0400_CP40_ET2000_orif_r1	Digiammonia	300	1	1	1	400	40				1	500	2000	Diesel	N2
Digiammonia_300_p01_P0400_CP40_ET2000_orif_r2	Digiammonia	300	1	1	2	400	40				1	500	2000	Diesel	N2
Digiammonia_300_p02_P0600_CP40_ET2000_orif_r1	Digiammonia	300	2	1	1	600	40				1	500	2000	Diesel	N2
Digiammonia_300_p02_P0600_CP40_ET2000_orif_r2	Digiammonia	300	2	1	2	600	40				1	500	2000	Diesel	N2
Digiammonia_300_p03_P0800_CP40_ET2000_orif_r1	Digiammonia	300	3	1	1	800	40				1	500	2000	Diesel	N2
Digiammonia_300_p03_P0800_CP40_ET2000_orif_r2	Digiammonia	300	3	1	2	800	40				1	500	2000	Diesel	N2

Figure 4.1: Excel datasheet.

Magnetinjektor V2

The pulse parameters are loaded to this software, specifying the energizing time and injection frequency. The ICU sends the pulse to the GENOTEC, which then sends the commands to the injector.

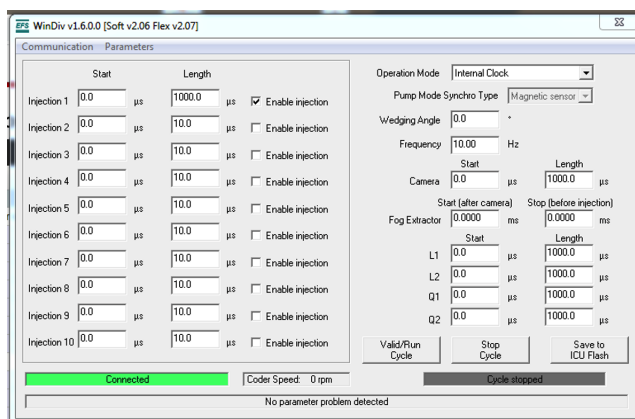


Figure 4.2: ICU controller.

YOKO DL716 Software

This program connects the computer to the data acquisition device. Here the channel configurations and the number of repetitions per sample are configured. It also records the raw data files on the computer for further processing.



Figure 4.3: YOKO DL716 software.

MATLAB. Xtasutiles.

Xtasutiles is a MATLAB script developed at CMT for processing raw data obtained from the YOKO. This program converts YOKO files into CSV files, rearranging the data into columns, which makes it easier to plot and compare with other datasets. Additionally, it allows for modifications to the original dataset through linear operations.



Figure 4.4: Xtasutiles in MATLAB.

High pressure pump controller.

This software is specifically designed to control the piston pump for the CMT. To set a desired pressure, it is needed to input the inlet air pressure. Given that the compression ratio is approximately ten to one, the input pressure must be adjusted until the desired output pressure value is achieved.



Figure 4.5: Pump controller.

Temperature recorder

All thermocouples are connected to this data acquisition program, allowing to visualize temperature variations in real time and obtain an average value for each experimental period.

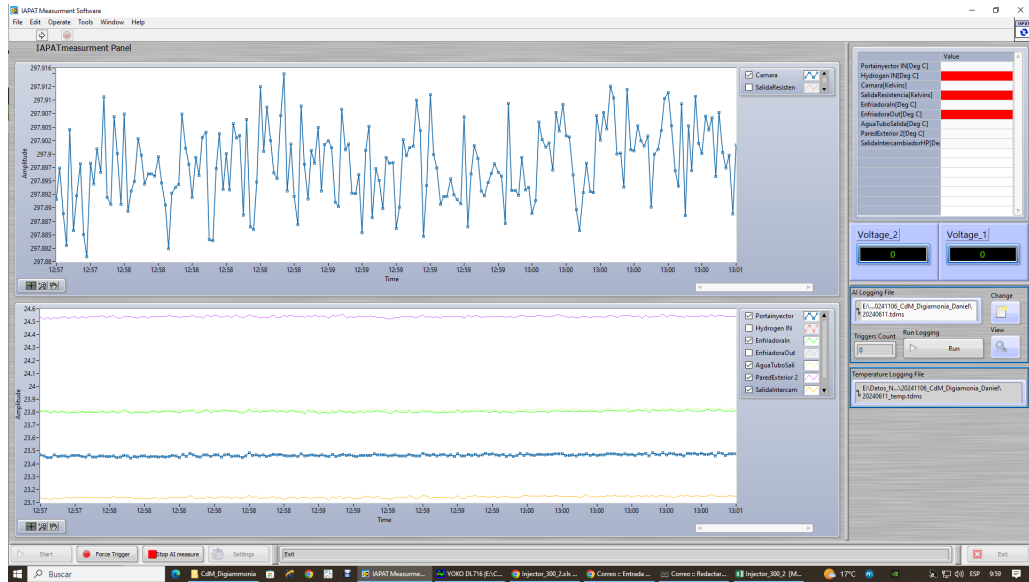


Figure 4.6: Temperature recorder.

4.2 Momentum flux signal obtention.

To measure the signal, the following conditions must be set to the operating point desired:

- Injection pressure.
- Back pressure.
- Energising time.

The injection frequency can be modified in case is needed to maintain a constant pressure in the common rail.

Subsequently, the YOKO screen have to be be cleared and to confirm that all objective values are stable before starting the measurements.

After recording the measurements on the computer through the YOKO software, the pressure values and temperature must be registered in the designated excel file for the experiment.

In figure 4.7 we see the momentum flux signal of the 50 measurements in one of the operating points.

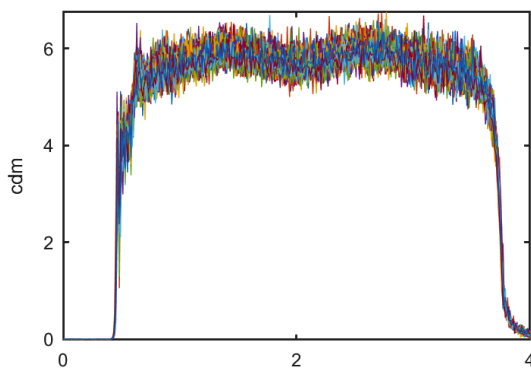


Figure 4.7: 50 momentum flux signals.

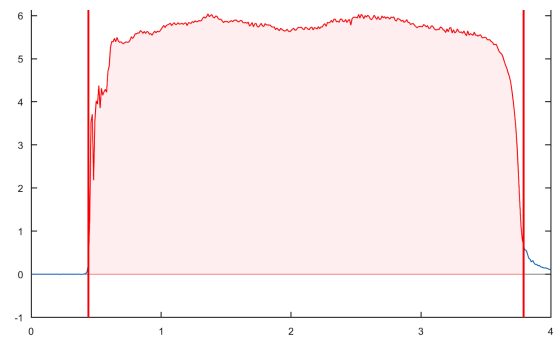


Figure 4.8: Average signal.

After a simple processing the average signal is obtained, see figure 4.8. The area under the curve represents the total momentum of the fuel jet during the injection.

4.3 Cumulative phenomena.

The obtained signal increases steadily throughout the injection event. However, the injection pressure is decreasing as shown on the pressure evolution graph in figure 4.9.

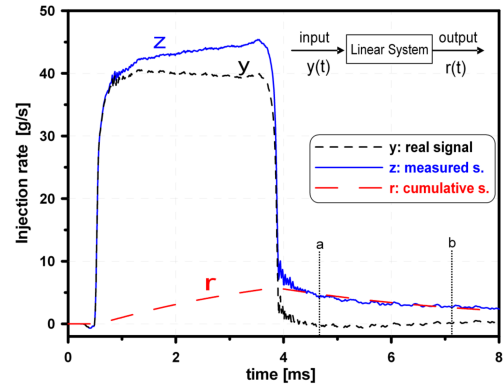
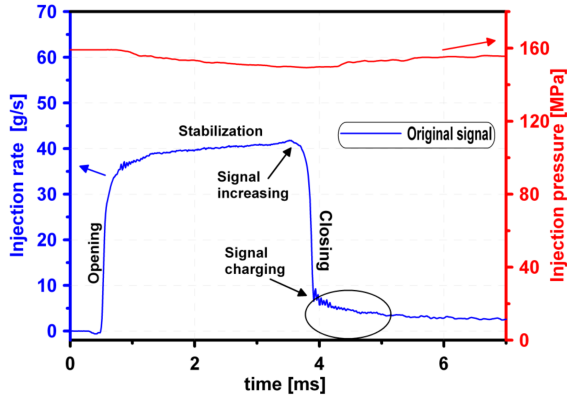


Figure 4.9: Cumulative phenomena [55]. **Figure 4.10:** Signal correction [55].

When the injection is over, the signal does not recover the initial value, indicating an unreal value of momentum flux. At the end of the injection, the nozzle is completely closed and the momentum flux should be zero.

The correction methodology for signal cumulative phenomena in injection rate measurements uses numerical solutions and iterative techniques to isolate and remove external influences from the measurement signal, see figure 4.10. By considering the measured signal as a combination of the true injection rate and a cumulative component, this approach calculates correction factors iteratively. This ensures the corrected signal accurately represents the actual injection process, thereby improving the reliability of similar measurements. This technique is presented in detail in the bibliography [55][18].

Once the cumulative phenomena has been rectified, the corrected signal can be used for subsequent processing.

4.4 Testing plan.

The experimental campaign was divided in two rounds based on the fuel employed for the experiments.

For the first campaign, the experiments were performed using diesel, with nine operating points defined in table 4.1.

For these hydraulic measurements, the temperature of the discharge chamber is close to that of the ambient (around 293 K) and the body of the injector is temperature-controlled to match that measured during previous experiments to 16 °C (289 K).

Fuel	Diesel–Ammonia
Injector nozzle diameter	250 μ m–300 μ m
<i>Momentum flux measurements</i>	
<i>Energising Time(ET) (μs)</i>	2000
<i>Injection pressure (bar)</i>	450–500–600–800
<i>Back – pressure (bar)</i>	40–50–60
<i>Injector return pressure (bar)</i>	0–8

Table 4.1: Testing plan matrix.

In the second campaign, the measurements will be performed using ammonia, maintaining the operating points in table 4.1. For ammonia, the injector holder is refrigerated close to 15°C (288 K), trying to keep ammonia in the liquid phase during the injection event.

On each operating point, fifty injections will be recorded to have a broader data sample. Although the common rail system can inject at pressures up to 2200 bar, with ammonia, the maximum pressure possible was lower to ensure stability and prevent phase changes (evaporation-cavitation phenomena).

Chapter 5

Results and Discussion.

In this chapter, the results of the momentum measurements for both fuels, diesel (base case) and ammonia, are presented.

All sections in this chapter present the results for both injectors with diameters of $250\mu\text{m}$ and $300\mu\text{m}$. Due to a limitation of the pressure sensor, we could not follow the entire test plan. The plan stipulated testing the injection at back-pressures of 40, 50, and 60 bar, but we were only able to measure at 40 bar.

5.1 Base case. Diesel as fuel.

As aforementioned in Chapter 2, diesel can be characterised using a flow meter, providing a reliable measurement of the mass flow rate at specific points. By comparing the results from these measurements with the momentum flux measurements, it can be verified the direct correlation between these two measurements. The process of measuring the rate of injection is not specified here as it is outside the scope of this project.

The graphs in figure 5.1 represent the measurements of the mass flow rate and the momentum flux.

For both diameters, a similar trend is observed in both momentum and rate of injection. Analysing a single diameter, it can be seen that the injection time is similar. However, for both injector sizes, the nozzle closes almost half a second earlier in the rate measurement at 400 bar.

It is important to note that in the momentum measurements, the injection occurs into a gas, while in the rate measurements, the injector is submerged in diesel. This, combined with the fact that the selected injector is designed to work at higher injection pressures, might explain the premature end of injection at 400 bar.

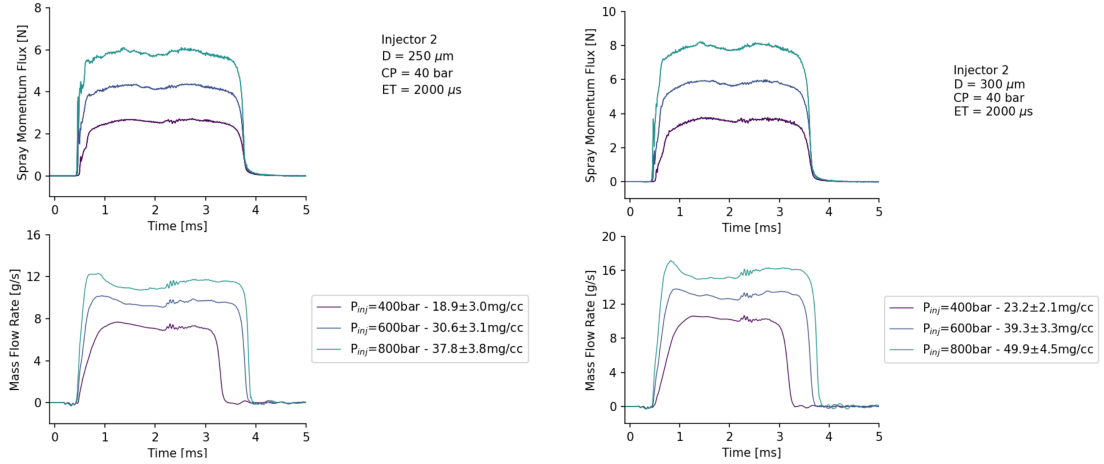


Figure 5.1: Rate of injection vs momentum flux signals for diesel of both injectors.

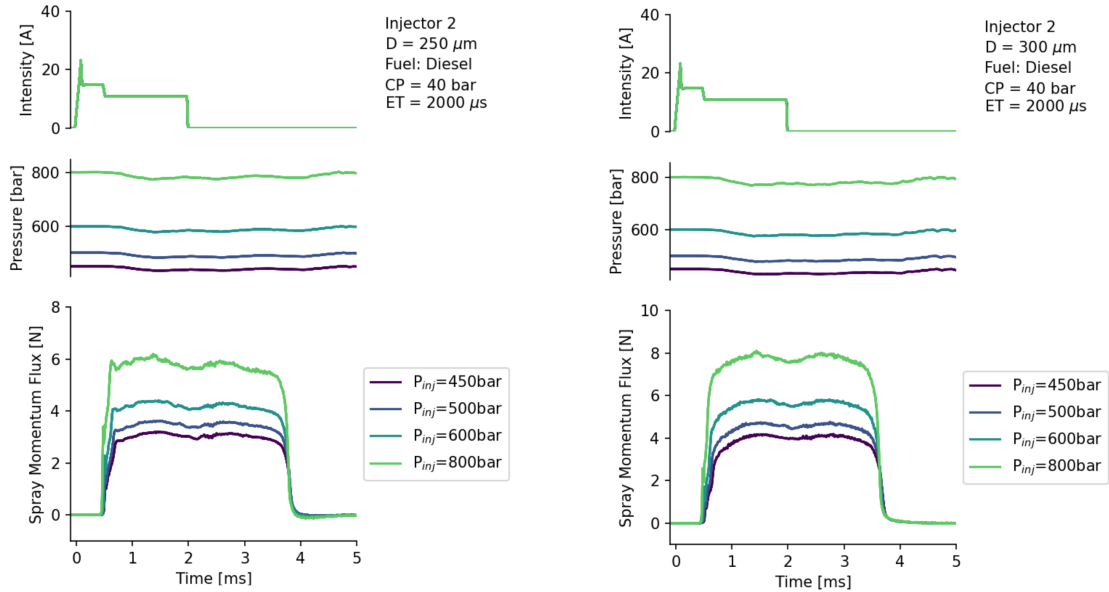


Figure 5.2: Momentum flux signals of diesel for both injectors.

Figure 5.1 & 5.2 show that the momentum flux and rate of injection measurements are very stable for both injectors. It is observed that the $300\mu\text{m}$ injector shows higher values for both momentum flux and rate at the same injection pressures, which is consistent with the larger diameter of the injection orifice, allowing a greater fluid flow through the injector.

5.2 Ammonia as fuel.

This section presents the ammonia measurements. Since the operation of the flow meter is not compatible with the ammonia properties, the results are focused on the momentum flux.

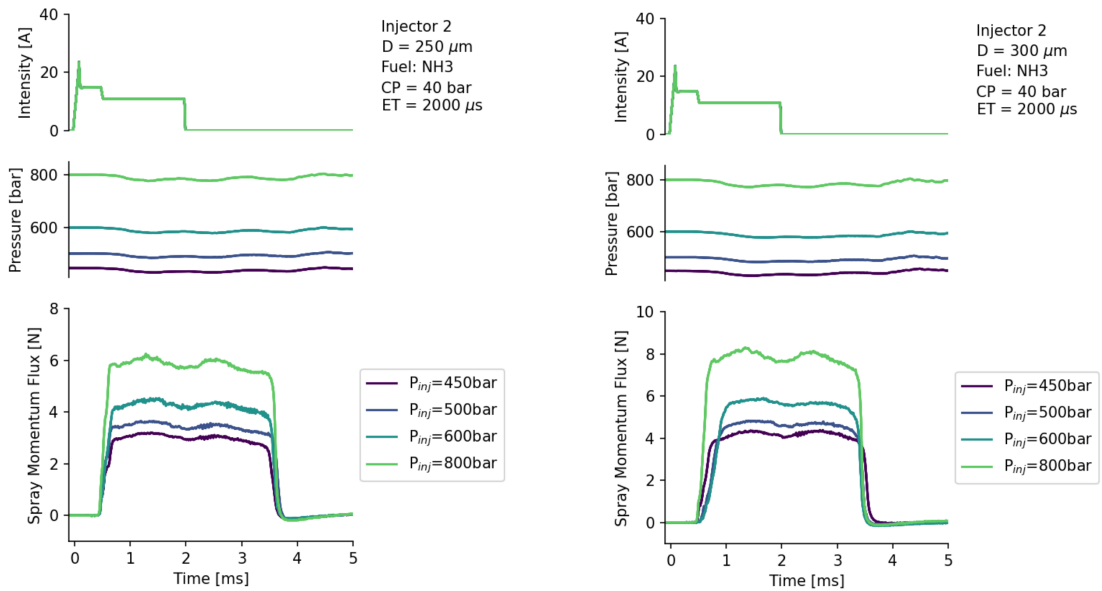


Figure 5.3: Momentum flux signals of ammonia for both injectors.

Figure 5.3 shows that ammonia exhibits stable behaviour throughout the injection process at all pressure values. It is noted that that the opening slopes present differences for the $300\mu\text{m}$ nozzle, while the opening slopes for the $250\mu\text{m}$ nozzle are homogeneous. The initial fluctuation in the injection could be related to the viscosity of liquid ammonia. Although the presence of instabilities in the opening slopes, the figure shows that the momentum flux value at steady state increases with the injection pressure.

Higher momentum flux values for the $300\mu\text{m}$ nozzle are also observed in this analysis. It should be mentioned that during the $300\mu\text{m}$ nozzle experiment, the

target fell off the sensor while injecting, which might have contributed to an error in the results.

5.3 Parametric analysis.

Figures 5.4 & 5.5 show a comparative analysis of diesel and ammonia momentum flux through the injectors diameters of $250\mu\text{m}$ and $300\mu\text{m}$. This analysis focuses on variations in spray momentum flux for both fuels under different injection pressures.

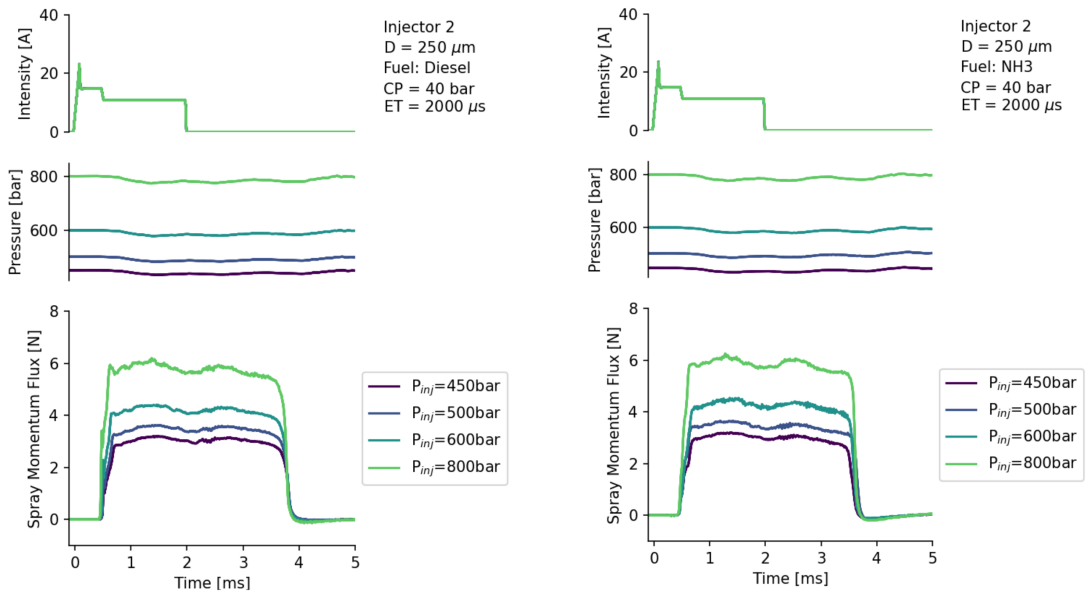


Figure 5.4: Momentum flux signals for $250\mu\text{m}$ injector of diesel and NH_3 .

For the $250\mu\text{m}$ injector diameter, it is evident that increasing injection pressure significantly impact the behaviour of both diesel and ammonia.

The spray momentum flux for the $250\mu\text{m}$ injector provides a more detailed comparison. At an injection pressure of 450 bar, both fuels exhibit a similar initial rise in spray momentum flux, reaching a peak before stabilising. With increasing injection pressure, the peak spray momentum flux also rises for both fuels. Diesel shows a slightly higher peak momentum flux compared to ammonia across all injection pressures.

Switching to the $300\mu\text{m}$ injector diameter, the overall trends observed with the $250\mu\text{m}$ injector persist, but with some notable differences. The pressure profiles for both fuels again show stability across varying injection pressures, with ammonia maintaining slightly lower pressure levels than diesel.

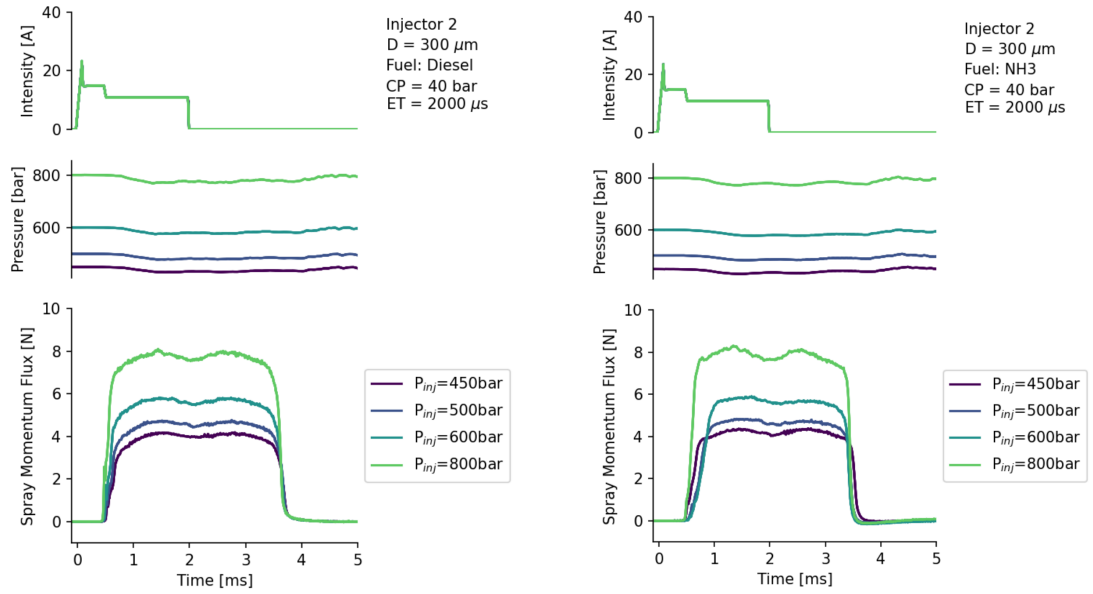


Figure 5.5: Momentum flux signals for 300 μ m injector of diesel and NH₃.

The spray momentum flux for the 300 μ m injector exhibits similar characteristics to the 250 μ m injector, with both fuels showing increased momentum flux at higher injection pressures. Diesel continues to demonstrate a higher peak flux compared to ammonia. The increased injector diameter amplifies the spray momentum flux for both fuels, indicating a direct correlation between injector size and spray development.

In summary, the parametric analysis across both injector sizes and fuels reveals consistent trends. Diesel generally exhibits similar spray momentum flux compared to ammonia, suggesting an analogous injection rate profile.

5.4 Further analysis of the results.

In this section a more precise analysis of the obtained results will be conducted.

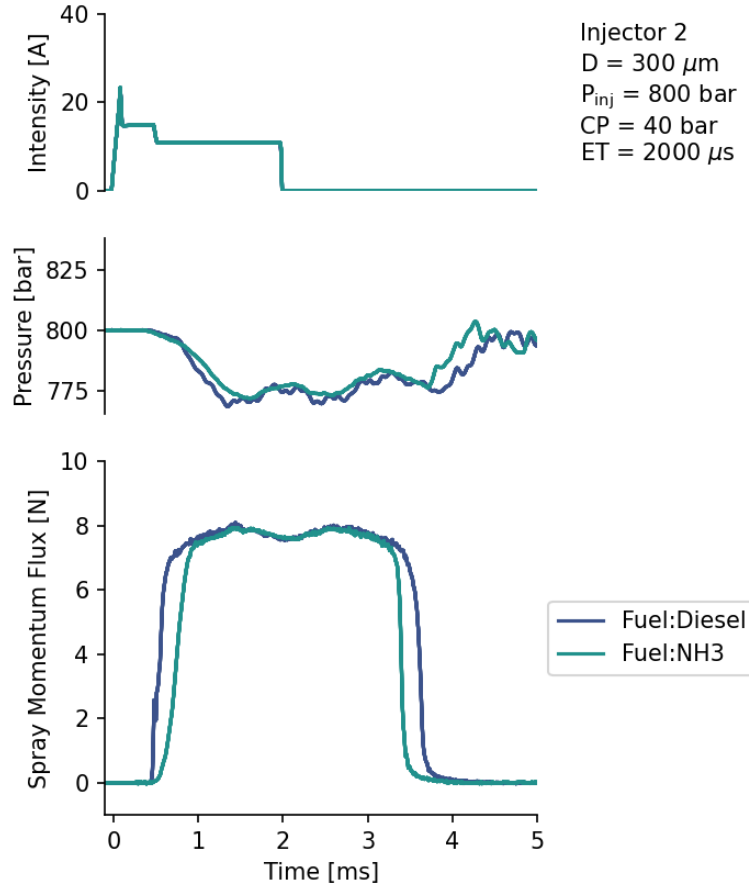


Figure 5.6: Overlaid momentum flux signals of diesel and ammonia.

Figure 5.6 is a direct comparison of both diesel and ammonia momentum flux measurements for an injection pressure of 800 bar.

Different conclusions can be drawn from these results. First, focusing on the 0.5 to 1 millisecond time-frame, it can be observed that the slopes of the momentum flux differ. The injection begins on the same instant, however, ammonia's jet seems to be delayed with respect to diesel. This behaviour can be attributed to the injector internal dynamics. Properties of ammonia, such as viscosity, density and vapor pressure differ from that of diesel. The injector needle mechanism is designed for diesel, hence the steep slope for this fuel at the beginning of the injection.

This hypothesis is supported by the behaviour of the momentum signal once the injection reaches steady-state conditions, 1.25 to 3.25 milliseconds in fig. 5.6. The momentum flux signal in the stabilized region of the injection for both fuels almost completely overlaps. This observation suggests that after overcoming the initial transient phase, the momentum flux value becomes independent of the fuel properties.

This conclusion is proved by the momentum flux definition (eq. 2.1). Considering that both fuels are incompressible, the mentioned equation yields:

$$\begin{aligned}
 \dot{M} &= u \cdot \dot{m} \\
 &= \sqrt{2 \cdot \frac{\Delta P}{\rho}} \cdot C_d \cdot A_o \cdot \rho \cdot \sqrt{2 \cdot \frac{\Delta P}{\rho}} \\
 &= C_d \cdot A_o \cdot \rho \cdot 2 \cdot \frac{\Delta P}{\rho} \\
 &= C_d \cdot A_o \cdot 2 \cdot \Delta P
 \end{aligned} \tag{5.1}$$

Being C_d the discharge coefficient, A_o the nominal nozzle area and ΔP the difference of pressure between the injection of the fuel and the back-pressure in the test-rig.

No term on the simplified equation depends on the fuel, but only on the experimental conditions.

Based on the obtained results, the observations made by Payri et al. [53] in their spray experiments are confirmed.

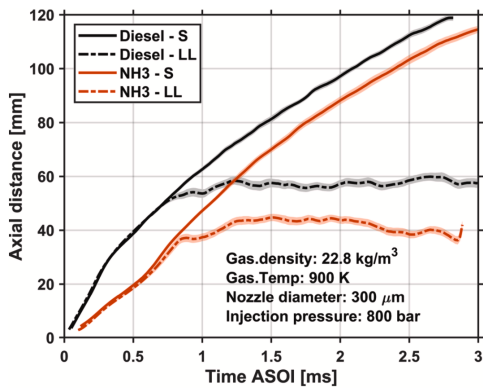


Figure 5.7: Rate of penetration.

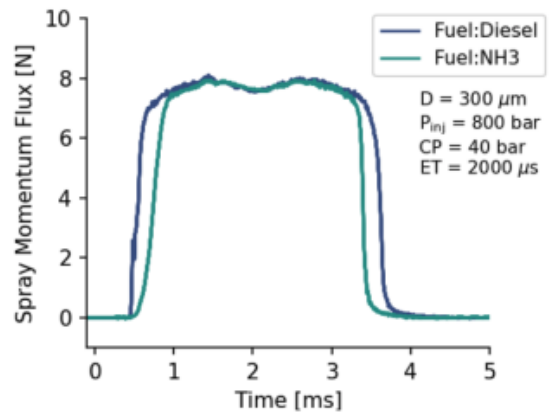


Figure 5.8: Momentum flux signals.

The aforementioned observations can be directly correlated with the spray penetration data presented Payri et al.

Two items can be underscored:

- At the beginning of the injection (from 0 to 1 ms in fig 5.7) ammonia shows a lower penetration rate. This anomaly in the experimental data is now understood with the results of this project. The slowdown matches with the gentler slope of the momentum flux signal in the same timeframe (fig 5.8). Confirming that the injector needle dynamics actually influence the injection spray behaviour.
- On the steady-state region (from 1.25 to 3.25 ms in fig 5.7) it can be observed a constant slope for the rate of penetration of both fuels. This proves the direct correlation of momentum flux and spray penetration, completely aligning with the momentum flux behavior in fig 5.8 (from 1.25 to 3 ms). The shift between both fuel lines in fig 5.7 is a product of the slower spray of ammonia, due to its characteristics.

5.5 Rate of injection inference from momentum flux measurements.

One of the main objectives of this project is to obtain the rate of injection (injected mass flow) for ammonia, since a direct measurement is not possible.

Firstly, the injector nozzle must be characterised. As presented in the Literature Review (Chapter 2) determining the discharge coefficient (C_d) of the nozzle is a key constant for fulfilling the objective. However, for ammonia it is considered the momentum flux equivalent, the momentum coefficient (C_m).

$$\overline{\dot{M}}_{experimental} = C_m \cdot \dot{M}_{theoretical} \quad (5.2)$$

$\overline{\dot{M}}$ is the average momentum flux value. Combining equation 5.2 with the definition of the momentum flux (eq. 2.1) the equation for the momentum coefficient is obtained:

$$C_m = \frac{\overline{\dot{M}}_{experimental}}{2 \cdot A_o \cdot \Delta P} \quad (5.3)$$

Recurring to equation 2.3 in Chapter 2, including a slight modification, the experimental rate of injection formula is:

$$\overline{m}_{experimental} = \sqrt{A_o \cdot \rho_f \cdot C_{d/m} \cdot \overline{M}_{experimental}} \quad (5.4)$$

By including the discharge coefficient, or its equivalent, the effective area of the nozzle is being considered in the formula, instead of the nominal value. This is an important remark, since the yielded result will be compared with experimental data.

5.5.1 Base case.

To infer data values using results from the formula, it is necessary to create a reference framework with diesel as the base case. The formula results will be compared with experimental measurements of rate of injection (ROI) of diesel. The ROI data is obtained from experiments conducted in the CMT. Two operating points will be considered throughout the analysis.

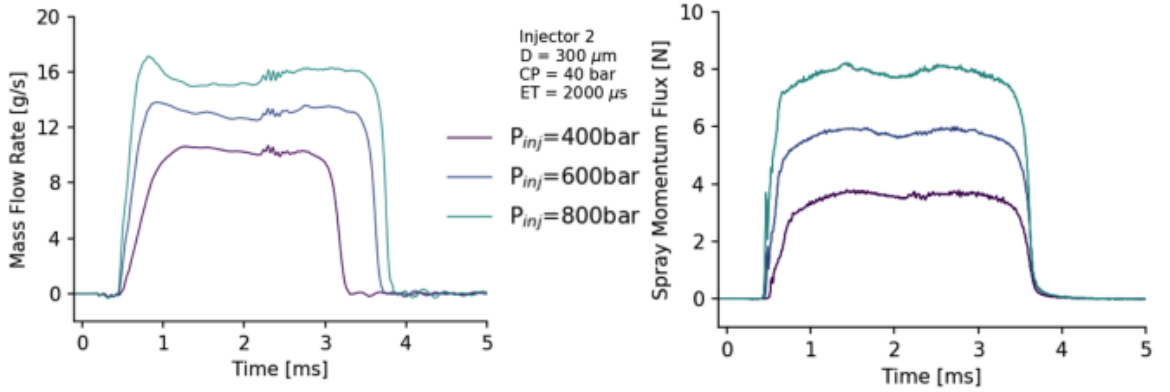


Figure 5.9: ROI and momentum flux signals for diesel.

The average momentum flux (\overline{M}) is obtained computing the average momentum flux signal of the studied operating points.

POINT			P_inj_ROI	ROI	P_inj_mflux	BP_mflux	Fuel_dens	C_d	Mflux
Nozzle diam.	Inj_P	BP							
μm	bar	bar	bar	g/s	bar	bar	kg/m ³	-	N
300	600	40	557.35	13.36	581.74	40.70	829.3558	0.6458	5.5850
300	800	40	759.149	16.1723	777.93	41.20	828.1154	0.6630	7.6729

Table 5.1: Diesel ROI and momentum flux data.

ROI_exp	Mflux_exp	ROI_theo	C_m	Error
g/s	N	g/s	-	%
13.3604	5.5850	14.5409	0.7649	8.8357
16.1723	7.6729	17.2567	0.7549	6.7049

Table 5.2: Diesel results.

The experimental deviation falls below the 10% threshold, demonstrating that the proposed methodology for determining the ROI value is both accurate and reliable.

5.5.2 Ammonia rate of injection.

Once that the framework is established, inferring ROI values for ammonia injection is the following step.

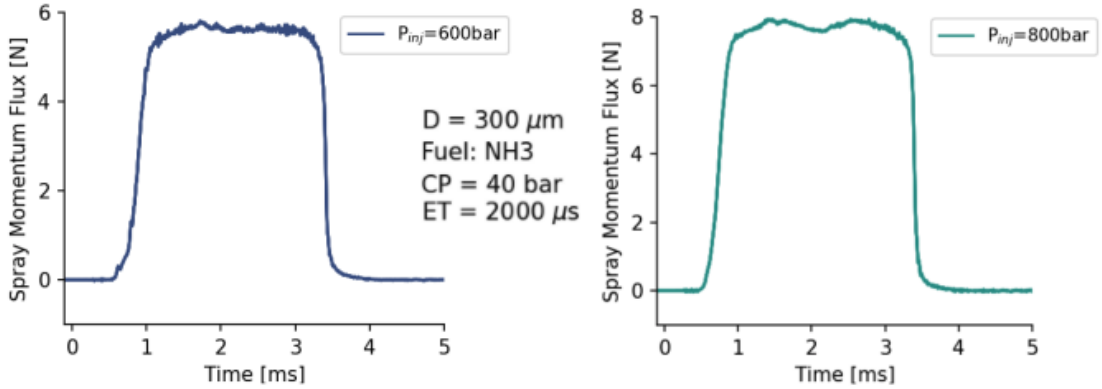


Figure 5.10: Momentum flux signals of two different operation points with ammonia.

The deviation value presented in the results table is referred to the theoretical ROI of diesel when injecting under the same conditions (injection pressure, back pressure and temperature).

POINT							
Nozzle diam.	Inj_P	BP	Inj_Temp	P_inj_mflux	BP_mflux	Fuel_dens	Mflux
μm	bar	bar	$^{\circ}C$	bar	bar	kg/m^3	N
300	600	40	22.90	583.6843	40.40	612	5.3727
300	800	40	22.70	780.4603	41.10	615	7.3425

Table 5.3: Ammonia momentum flux data.

ROI_diesel_theo	Mflux_exp	C_m	ROI_nh3_theo	Deviation
g/s	N	-	g/s	%
14.5409	5.5850	0.6995	12.7509	12.3101
17.2567	7.6729	0.7025	14.9740	13.2279

Table 5.4: Ammonia results.

The obtained results confirm what was expected. The slightly lower crest of momentum flux, in addition to the late needle opening and early closing result in lower mass flow rate injected. These results also confirm that for a higher injection pressure, higher momentum flux, and consequently higher mass injected.

Chapter 6

Conclusions and further development.

6.1 Conclusions.

The primary focus of this project was the re-design of the test rig and the installation set-up to accommodate the use of ammonia as a fuel. The modifications made to the existing momentum flux test rig were needed to ensure its compatibility with ammonia. The re-design involved key changes, including the adaptation of gaskets, pipes and discharge system to withstand ammonia's corrosive and toxic nature.

The experimental set-up and methodology employed in this study proved to be effective in achieving the project's objectives. The test-rig allowed for precise measurement of the spray momentum flux of both diesel and ammonia under various conditions. This experimental approach provided valuable data, demonstrating ammonia stable injection characteristics. Despite the challenges posed by ammonia's properties, this project has shed light on its potential as a sustainable diesel-like fuel alternative, regarding injection spray behaviour.

One significant finding during the experimentation was that ammonia deteriorates EPDM o-rings, necessitating their frequent replacement. This led to a shortage of spare parts, pointing out the need for maintaining an extra security stock of these components for future operations.

The comparative analysis of diesel and ammonia revealed that both fuels exhibit similar trends in spray momentum flux across different injector sizes and injection pressures. The overall behaviour was consistent, suggesting that with appropriate injectors and supporting technology, ammonia could be used without significant performance loss. The influence of injector diameter on spray momentum flux was also highlighted, with larger injector nozzle resulting in higher momentum flux for both fuels.

It was also observed that the dynamics of the injector needle impact the performance of the injected spray. Furthermore, it was confirmed that the momentum flux of a steady-state spray remains independent of the fuel properties. Additionally, the research validated that the momentum flux has a direct correlation to the mass of the injected fuel and its dependence on the injection pressure.

The successful modifications to the test-rig and the reliability of the experimental methodology represent significant advancements in the study of ammonia as a fuel. The project has laid a solid foundation for further exploration into ammonia dynamics inside the injector and the spray behaviour, contributing to the broader goal of decarbonising the transport and energy generation industries.

6.2 Further developments.

This project sets the ground for the development of ammonia injection studies. Going forward, different aspects will be addressed:

- Improvements in the installation. Acquisition of pressure sensors that allow measurements above 40 bar. This will enable the measurement of all points in the test plan and provide more data for reaching more precise conclusions.
- Hydraulic characterisation of injectors working with ammonia as a fuel.
- Data analysis and determination of the mass flow rate of injected ammonia based on momentum flux rate and rate of injection data.
- Obtaining a correlation algorithm that links the rate of injection (ROI) of diesel to the rate of injection of ammonia by comparing the ROI and momentum flux data for diesel, and generating a model to translate the momentum flux data of ammonia to the ROI for ammonia based on the diesel data.
- Development of CFD models based on the characterisation of the injectors.

Bibliography

- [1] *Why Milankovitch (Orbital) Cycles Can't Explain Earth's Current Warming*. URL: <https://science.nasa.gov/science-research/earth-science/why-milankovitch-orbital-cycles-cant-explain-earths-current-warming/> (cit. on p. 2).
- [2] Meijia Shan. «Analysis on the Influence of Doubled Carbon Dioxide on the Extreme Weather». In: *Applied and Computational Engineering* 3 (May 2023), pp. 368–373. DOI: 10.54254/2755-2721/3/20230554 (cit. on pp. 2, 3).
- [3] *How do we know climate change is happening? | Grantham Institute – Climate Change and the Environment | Imperial College London*. URL: <https://www.imperial.ac.uk/grantham/publications/climate-change-faqs/how-do-we-know-climate-change-is-happening/> (cit. on pp. 2, 4).
- [4] *Understanding Global Warming Potentials | US EPA*. URL: <https://www.epa.gov/ghgemissions/understanding-global-warming-potentials> (cit. on p. 3).
- [5] U.S. Global Change Research Program. «Climate science special report: Fourth national climate assessment, volume I». In: *U.S. Global Change Research Program* 1 (2018). Ed. by D.J. Wuebbles, D.W. Fahey, K.A. Hibbard, D.J. Dokken, B.C. Stewart, and T.K. Maycock, p. 470. ISSN: 0736-6825. DOI: 10.7930/J0J964J6. URL: <https://www.epa.gov/climate-indicators/climate-change-indicators-atmospheric-concentrations-greenhouse-gases> (cit. on p. 3).
- [6] *Net Zero Emissions by 2050 Scenario (NZE) – Global Energy and Climate Model – Analysis - IEA*. URL: <https://www.iea.org/reports/global-energy-and-climate-model/net-zero-emissions-by-2050-scenario-nze> (cit. on p. 3).
- [7] *Atmospheric greenhouse gas concentrations*. URL: <https://www.eea.europa.eu/en/analysis/indicators/atmospheric-greenhouse-gas-concentrations> (cit. on p. 3).

- [8] *The global energy landscape to 2050: Emissions* / McKinsey. URL: <https://www.mckinsey.com/industries/oil-and-gas/our-insights/charting-the-global-energy-landscape-to-2050-emissions> (cit. on pp. 3, 4).
- [9] *What is the Kyoto Protocol?* / UNFCCC. URL: https://unfccc.int/kyoto_protocol (cit. on p. 5).
- [10] *The Paris Agreement* / United Nations. URL: <https://www.un.org/en/climatechange/paris-agreement> (cit. on p. 5).
- [11] *International Agreements on Climate Change - Iberdrola*. URL: <https://www.iberdrola.com/sustainability/international-agreements-on-climate-change> (cit. on p. 5).
- [12] *The European Green Deal - European Commission*. URL: https://commission.europa.eu/strategy-and-policy/priorities-2019-2024/european-green-deal_en (cit. on p. 5).
- [13] *THE 17 GOALS* / Sustainable Development. URL: <https://sdgs.un.org/goals> (cit. on p. 6).
- [14] *Transport and mobility EU*. URL: <https://www.eea.europa.eu/en/topics/in-depth/transport-and-mobility> (cit. on p. 7).
- [15] *Energy Statistics Data Browser – Data Tools - IEA*. URL: <https://www.iea.org/data-and-statistics/data-tools/energy-statistics-data-browser?country=WORLD&fuel=Energy%20supply&indicator=TESbySource> (cit. on p. 7).
- [16] *Transport in Transition*. URL: <https://www.dnv.com/publications/transport-in-transition-242808/> (cit. on p. 7).
- [17] *The Potential of E-fuels to Decarbonise Ships and Aircraft* / ITF. URL: <https://www.itf-oecd.org/potential-e-fuels-decarbonise-ships-aircraft> (cit. on pp. 7, 12, 15).
- [18] Jaime Gimeno García. «Desarrollo y aplicación de la medida del flujo de cantidad de movimiento de un chorro Diesel». PhD thesis. Valencia (Spain): Universitat Politècnica de València, June 2008. DOI: 10.4995/Thesis/10251/8306. URL: <https://riunet.upv.es/handle/10251/8306> (cit. on pp. 8, 25, 26, 30, 32, 35, 57).
- [19] *WebCMT*. URL: <https://www.cmt.upv.es/#/> (cit. on p. 9).
- [20] R. D. Reitz et al. «IJER editorial: The future of the internal combustion engine». In: *International Journal of Engine Research* 21.1 (Jan. 2020), pp. 3–10. ISSN: 20413149. DOI: 10.1177/1468087419877990 (cit. on pp. 11, 12).

- [21] Ameya Joshi. «Review of Vehicle Engine Efficiency and Emissions». In: *SAE International Journal of Advances and Current Practices in Mobility* 2.5 (Apr. 2020), pp. 2479–2507. ISSN: 01487191. DOI: 10.4271/2020-01-0352. URL: <https://www.sae.org/publications/technical-papers/content/2020-01-0352/> (cit. on p. 11).
- [22] Rohan Challa, Dipti Kamath, and Annick Anctil. «Well-to-wheel greenhouse gas emissions of electric versus combustion vehicles from 2018 to 2030 in the US». In: *Journal of environmental management* 308 (Apr. 2022). ISSN: 1095-8630. DOI: 10.1016/J.JENVMAN.2022.114592. URL: <https://pubmed.ncbi.nlm.nih.gov/35121453/> (cit. on p. 12).
- [23] Panagiotis Karvounis, Charalampos Tsoumpris, Evangelos Boulougouris, and Gerasimos Theotokatos. «Recent advances in sustainable and safe marine engine operation with alternative fuels». In: *Frontiers in Mechanical Engineering* 8 (Nov. 2022). ISSN: 22973079. DOI: 10.3389/FMECH.2022.994942 (cit. on p. 12).
- [24] *What are biofuels? Types and main advantages | Repsol*. URL: <https://www.repsol.com/en/technology-and-digitalization/technology-lab/emissions-reduction/biofuels/index.cshtml> (cit. on p. 12).
- [25] Herry Lesmana, Zhezi Zhang, Xianming Li, Mingming Zhu, Wenqiang Xu, and Dongke Zhang. «NH₃ as a transport fuel in internal combustion engines: A technical review». In: *Journal of Energy Resources Technology, Transactions of the ASME* 141.7 (July 2019). ISSN: 15288994. DOI: 10.1115/1.4042915/725857. URL: <https://dx.doi.org/10.1115/1.4042915> (cit. on pp. 13, 15, 17).
- [26] Cinzia Tornatore, Luca Marchitto, Pino Sabia, and Mara De Joannon. «Ammonia as Green Fuel in Internal Combustion Engines: State-of-the-Art and Future Perspectives». In: *Frontiers in Mechanical Engineering* 8 (July 2022), p. 944201. ISSN: 22973079. DOI: 10.3389/FMECH.2022.944201/BIBTEX (cit. on pp. 13, 14).
- [27] «Ammonia: zero-carbon fertiliser, fuel and energy store POLICY BRIEFING». In: (2020) (cit. on pp. 13, 20).
- [28] João Sousa Cardoso, Valter Silva, Rodolfo C. Rocha, Matthew J. Hall, Mário Costa, and Daniela Eusébio. «Ammonia as an energy vector: Current and future prospects for low-carbon fuel applications in internal combustion engines». In: *Journal of Cleaner Production* 296 (May 2021), p. 126562. ISSN: 09596526. DOI: 10.1016/j.jclepro.2021.126562. URL: <https://linkinghub.elsevier.com/retrieve/pii/S0959652621007824> (cit. on p. 14).

- [29] Nitrogen+syngas. «Sustainable ammonia for food and power». In: *Nitrogen+syngas* 354 (2018), pp. 6–7. URL: www.nitrogenandsyngas.com%20https://bcinsight.com//nitrogen_syngas.asp (cit. on pp. 14, 20).
- [30] *Report for pilot “Ammonia as Fuel”*. URL: <https://grontskipsfartsprogram.no/wp-content/uploads/2022/03/Ammonia-as-fuel-final-rev.pdf> (cit. on pp. 15, 19).
- [31] Rafael Estevez, Francisco J. López-Tenllado, Laura Aguado-Deblas, Felipa M. Bautista, Antonio A. Romero, and Diego Luna. «Current Research on Green Ammonia (NH₃) as a Potential Vector Energy for Power Storage and Engine Fuels: A Review». In: *Energies* 2023, Vol. 16, Page 5451 16.14 (July 2023), p. 5451. ISSN: 1996-1073. DOI: 10.3390/EN16145451. URL: <https://www.mdpi.com/1996-1073/16/14/5451/htm%20https://www.mdpi.com/1996-1073/16/14/5451> (cit. on pp. 15, 18).
- [32] by Abs. «Potential of Ammonia as Fuel in Shipping». In: (2022). ISSN: 2021/2022. URL: www.emsa.europa.eu%20https://cedelft.eu/wp-content/uploads/sites/2/2022/12/CE_Delft_EMSA_210113_Ammonia-as-fuel-in-Shipping_FINAL.pdf (cit. on p. 15).
- [33] Pavlos Dimitriou and Rahat Javaid. «A review of ammonia as a compression ignition engine fuel». In: *International Journal of Hydrogen Energy* 45.11 (Feb. 2020), pp. 7098–7118. ISSN: 0360-3199. DOI: 10.1016/J.IJHYDENE.2019.12.209 (cit. on pp. 16, 18).
- [34] Krister A. Pedersen, Michał T. Lewandowski, Corinna Schulze-Netzer, Michał Pasternak, and Terese Løvås. «Ammonia in Dual-Fueled Internal Combustion Engines: Impact on NO_x, N₂O, and Soot Formation». In: *Energy and Fuels* 37.22 (Nov. 2023), pp. 17585–17604. ISSN: 15205029. DOI: 10.1021/ACS.ENERGYFUELS.3C02549/ASSET/IMAGES/LARGE/EF3C02549{_}0019.JPEG. URL: <https://pubs.acs.org/doi/full/10.1021/acs.energyfuels.3c02549> (cit. on pp. 17, 18).
- [35] *MAN B&W ammonia engine development*. URL: <https://www.man-es.com/marine/products/two-stroke-engines/ammonia-engine?592380e5-7b22-42aa-bf83-f8dd18223552%5B%5D=0> (cit. on pp. 17, 18, 22).
- [36] Jorge Martins and F. P. Brito. «Alternative fuels for internal combustion engines». In: *Energies* 13.15 (Aug. 2020). ISSN: 1996-1073. DOI: 10.3390/EN13164086. URL: <https://repositorium.sdum.uminho.pt/handle/1822/66677> (cit. on p. 18).
- [37] IRENA International Renewable Energy Agency and Methanol Institute. «Innovation Outlook: Renewable Ammonia». In: *Innovation Outlook: Renewable Methanol* (2021), pp. 1–124 (cit. on p. 19).

- [38] *West Fertilizer Explosion and Fire | CSB*. URL: <https://www.csb.gov/west-fertilizer-explosion-and-fire/> (cit. on p. 19).
- [39] Cinzia Tornatore, Luca Marchitto, Pino Sabia, and Mara De Joannon. «Ammonia as Green Fuel in Internal Combustion Engines: State-of-the-Art and Future Perspectives». In: *Frontiers in Mechanical Engineering* 8 (July 2022). ISSN: 22973079. DOI: 10.3389/FMECH.2022.944201/FULL (cit. on p. 19).
- [40] «AMMONIA TRANSPORT & STORAGE #2». In: (). URL: www.ptx-hub.org (cit. on p. 19).
- [41] Nick Ash and Tim Scarbrough. *Sailing on Solar - Could green ammonia decarbonise international shipping?* June 2019 (cit. on p. 20).
- [42] K. Machaj, J. Kupecki, Z. Malecha, A. W. Morawski, M. Skrzypkiewicz, M. Stanlik, and M. Chorowski. «Ammonia as a potential marine fuel: A review». In: *Energy Strategy Reviews* 44 (Nov. 2022), p. 100926. ISSN: 2211-467X. DOI: 10.1016/J.ESR.2022.100926 (cit. on pp. 20, 23).
- [43] *News - Clean marine: £5.5m research effort to fuel ships on green ammonia - University of Nottingham*. URL: <https://www.nottingham.ac.uk/news/clean-marine-5.5m-research-effort-to-fuel-ships-on-green-ammonia> (cit. on p. 21).
- [44] *ENGIMMONIA - Chair of Energy Systems*. URL: <https://www.epe.ed.tum.de/en/es/research/projects/engimmonia/> (cit. on p. 21).
- [45] *World's first full scale ammonia engine test - an important step towards carbon free shipping*. URL: <https://www.wartsila.com/media/news/30-06-2020-world-s-first-full-scale-ammonia-engine-test---an-important-step-towards-carbon-free-shipping-2737809> (cit. on p. 22).
- [46] *Wärtsilä to deliver ammonia fuel system for two EXMAR Medium size Gas Carriers*. URL: <https://www.wartsila.com/media/news/08-02-2024-wartsila-to-deliver-ammonia-fuel-system-for-two-exmar-medium-size-gas-carriers-3400531> (cit. on p. 22).
- [47] Martin Cames, Nora Wissner, and Jürgen Sutter. *Ammonia as a marine fuel*. Tech. rep. Berlin: Öko Institut, June 2021. URL: <https://en.nabu.de/imperia/md/content/nabude/verkehr/210622-nabu-study-ammonia-marine-fuel.pdf> (cit. on p. 22).
- [48] *Climate action and clean air in shipping*. URL: <https://www.imo.org/en/OurWork/Environment/Pages/Decarbonization%20and%20Clean%20air%20in%20shipping.aspx> (cit. on p. 23).
- [49] *FuelEU Maritime*. URL: <https://www.dnv.com/maritime/insights/topics/fueleu-maritime/> (cit. on p. 23).

- [50] Francisco Payri González and José M^a Desantes Fernández. *MOTORES DE COMBUSTIÓN INTERNA ALTERNATIVOS*. Editorial Universitat Politècnica de València, June 2011. ISBN: 978-84-8363-70. URL: <http://hdl.handle.net/10251/70998> (cit. on pp. 24–26).
- [51] *Bosch Common Rail Injectors Work Introduction - DIESELO*. URL: <https://www.dieselo.com/bosch-common-rail-injectors-work-introduction/> (cit. on p. 25).
- [52] Raul Payri, José M. García-Oliver, Gabriela Bracho, and Jiawei Cao. «Experimental characterization of direct injection liquid ammonia sprays under non-reacting diesel-like conditions». In: *Fuel* 362 (Apr. 2024), p. 130851. ISSN: 0016-2361. DOI: 10.1016/J.FUEL.2023.130851 (cit. on p. 27).
- [53] R. Payri, G. Bracho, J. A. Soriano, P. Fernández-Yáñez, and O. Armas. «Nozzle rate of injection estimation from hole to hole momentum flux data with different fossil and renewable fuels». In: *Fuel* 279 (Nov. 2020), p. 118404. ISSN: 0016-2361. DOI: 10.1016/J.FUEL.2020.118404 (cit. on pp. 32, 65).
- [54] *Engine Combustion Network – Engine Combustion Network*. URL: <https://ecn.sandia.gov/> (cit. on p. 46).
- [55] R. Payri, F. J. Salvador, J. Gimeno, and G. Bracho. «A new methodology for correcting the signal cumulative phenomenon on injection rate measurements». In: *Experimental Techniques* 32.1 (Jan. 2008), pp. 46–49. ISSN: 07328818. DOI: 10.1111/J.1747-1567.2007.00188.X. URL: https://www.researchgate.net/publication/229455021_A_new_methodology_for_correcting_the_signal_cumulative_phenomenon_on_injection_rate_measurements (cit. on p. 57).

Part II

TERMS OF REFERENCE

Chapter 7

General Conditions of the Injection Laboratory.

This chapter outlines all the essential needs and requirements for the room and the experimental setup. It also provides the basic rules for conducting work safely, ensuring the physical integrity and health of the operators. The rules outlined here are systematically checked to ensure compliance.

7.1 Experimental room conditions.

The test room refers to the space required for the momentum flux measurements. The conditions the test room must meet are as follows:

- Soundproofing: The room is acoustically isolated from the outside to dampen the generated noise. The walls also meet the minimum noise isolation requirements as per the building code (CTE DB HR).
- Ventilation: The test room has mechanical ventilation system with an exhaust capable of creating negative pressure in the room to extract possible leaks of ammonia.
- Fire Protection: The room is equipped with a fire protection system, including a 21A-113B efficiency extinguisher. The materials used in the room's construction meet the fire safety requirements (CTE DB SI). The room also has integrated fire detection sensors and ammonia leakage sensors.

- **Non-slip Flooring:** The test room has non-slip flooring to prevent falls.
- **Lighting and Electrical Protection:** The room has a power capacity of 25kW, illuminated by twelve 40W neon tubes grouped in four panels. The adjoining room is lit by six tubes in two panels. A circuit breaker protects the room from short circuits and power surges, and there are several power outlets with grounding.
- **Compressed Air Installation:** The room has a compressed air system with 1/2" pipes capable of handling the 8 bar of pressure supplied by a compressor located in an independent room.
- **Glycol Supply:** Refrigerated glycol is supplied from an external tank through circulation pumps. The installation pipes are of diameter 3/4" and made of galvanised iron, equipped with stop valves. The glycol supply to the injector holder and the ammonia intercooler is branched using translucent PVC pipes.
- **Dimensions and Boundaries:** The test room's dimensions are sufficient for maintenance, assembly, supervision, and operation. There is no direct connection to other rooms containing explosive materials. The pipe passages through floors, walls, and ceilings are sealed, and the room has a direct and short exit to an open area.
- **Access:** Access to unauthorised personnel is prohibited.

7.2 Installation conditions.

The experimental setup meets the following conditions:

- All components (test-rig, pneumatic pump, pipes, etc.) are mounted on anti-vibration supports.
- All wiring is not on the floor nor in common passage areas, to avoid tripping.
- Nitrogen bottles remain closed except during filling or emptying, where they are opened for the least time possible.
- Ammonia bottles are only opened after leak-proofing the installation with nitrogen, and the ventilation system is turned on.

7.3 Rules for operators.

Operators and personnel accessing the room during tests must follow these rules:

- Connect the ventilation system before starting tests.
- Tests must be conducted with the door closed to prevent unauthorised access and interruptions, and to minimise noise transmission to other areas.
- During tests, no personnel can be in the room. Doors must be kept closed and personnel in the adjacent room must be equipped with appropriate protective gear.

7.4 Recommendations for nitrogen use.

Recommendations for handling nitrogen include:

- Position the container to avoid tipping, damage, or heating. Do not store it near combustible substances, ensure its seal, and provide good ventilation.
- Use work gloves and safety shoes when handling the container.
- In case of a leak, vent nitrogen through the ventilation system. Nitrogen does not harm the environment but is dangerous in confined spaces due to oxygen displacement.

7.5 Recommendations for ammonia use.

Recommendations for handling ammonia include:

- Position the container to avoid tipping, damage, or heating. Do not store it near combustible substances, ensure its seal, and provide good ventilation.
- Use work gloves and safety shoes when handling the container.
- Must use full facepiece and a chemical protective suit for ammonia operation.
- In case of a leak, vent through the ventilation system. Ammonia must be directed to the acid trap. It is not permitted to vent directly to the atmosphere.

Chapter 8

Methodology for using the installation

This chapter describes the methodology for using the installation, including the start-up and shutdown sequences of the test rig and maintenance tasks to ensure the setup's proper conservation.

8.1 Start-up and shut-down sequences.

Start-up sequence

The start-up sequence involves the following steps:

1. Turn on the ventilation system.
2. Switch on all signal amplifiers at least 30 minutes before the first measurement.
3. Turn on the computer, the data acquisition device (YOKO), the injector control unit and the GENOTEC.
4. Open the pressurised air supply of the high pressure pneumatic pump.
5. Start up the control software and verify or set-up the data channels on the YOKO.

6. Turn on the glycol refrigeration system and the circulation pumps.
7. Set the desired back-pressure inside the test-rig regulating the nitrogen flow. Check the value both on the YOKO and the bottle manometer.
8. Set the pressure in the fuel return sleeve to 8 bar with compressed air.
9. Check for leaks.
10. Set the injection details on the software and start the measurements.

Shutdown sequence

The shutdown sequence involves the following steps:

1. Stop the injection and turn off the pneumatic pump.
2. Cut the air supply to the pump.
3. Depressurise the common rail by opening the valve on the accumulator.
4. Depressurise the test-rig from the upper valve, so it only drains the gases to the return line.
5. Drain the injected fuel in liquid form to the return line.
6. Depressurise the pipe between the nitrogen bottle and the manometer.
7. Close the air supply to the return sleeve.
8. Turn off the refrigeration system and close the glycol valves.
9. Turn off all electronic devices and signal amplifiers.
10. Turn off the ventilation system.

In the case of using ammonia as fuel, the pump start up is not straightforward. These are the steps to follow to correctly turn on the pump.

1. Open the pressurised air supply of the high pressure pneumatic pump.
2. Start the pump using diesel as fuel until it reaches steady state operation conditions.
3. Purge all diesel in the pump, accumulator and common rail with ammonia through the valve in the accumulator.
4. Close valves and regulate operation pressure with ammonia in the system.

Chapter 9

Installation maintenance.

9.1 Daily maintenance.

Daily maintenance tasks, performed before or after tests, are necessary for accurate results and setup conservation. They include:

- Before tests:
 - Visually inspect fuel and refrigeration lines for leaks.
 - Ensure that there is enough fuel for the experiment in the tanks.
 - Check electrical connections.
 - Check hydraulic connections.
 - Check that the ventilation system functions correctly.
- After tests:
 - Purge the completely the installation.
 - Complete a log indicating the test type and any incidents.

9.2 Periodic maintenance.

Periodic maintenance, done at longer intervals, includes:

- Disassembling and cleaning each test-rig component and replacement of gaskets.
- Replacing diesel filters every 1500 hours.
- Annually doing maintenance on the acid trap and calibrating the test-rig pressure and temperature sensors.

Part III

BUDGET

Chapter 10

BUDGET

In this chapter, the project costs are described. It presents the expenses for components purchased for assembly, the use of measurement equipment, the materials used, and the labor required to carry out the project.

The labor costs are detailed, including a university professor, a doctoral student, a laboratory technician, and an industrial engineering graduate.

The cost of the concepts related to the use of facilities and machinery has been calculated based on the depreciation of these assets over their useful life, considering that they operate 40 hours a week for 46 weeks a year. This approach ensures an accurate allocation of the operational costs to the project.

Furthermore, the cost of software licenses used has been considered. Although these licenses are also employed in the development of other projects, the total cost of the license has been allocated to the project to simplify the computations.

In addition to direct costs, indirect costs such as administrative expenses and utilities have been factored in to provide a complete financial overview.

On the next page a cost breakdown can be found.

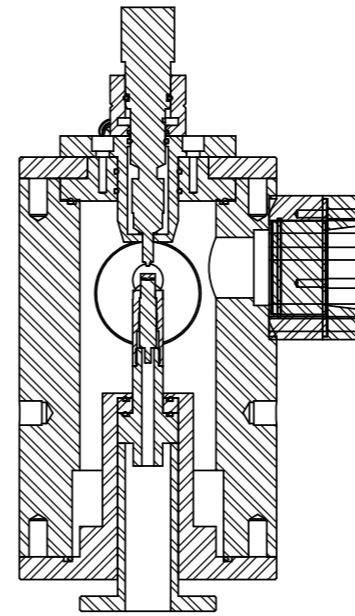
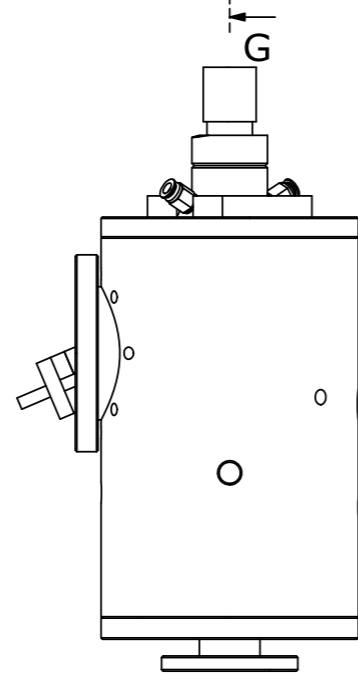
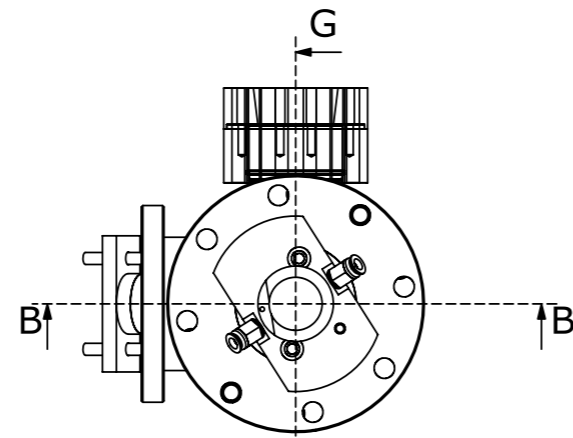
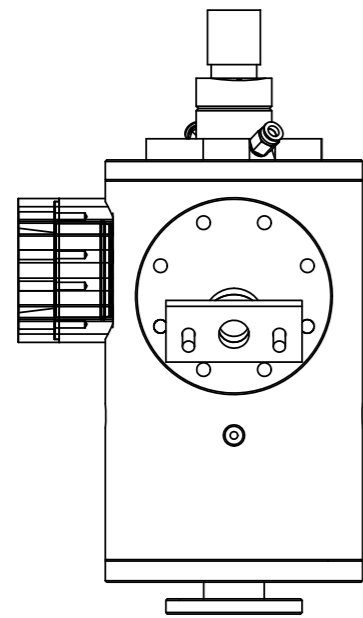
BUDGET

	Description	Measure	Units	Unitary Price	Amount	
UO1	Materials.				455.89	€
	O-RING FKM75 23.00 1.55	8	Units	3.25	26.00	
	O-RING FKM75 24.60 3.00	8	Units	5.47	43.76	
	O-RING FKM75 61.00 2.00	3	Units	9.05	27.15	
	O-RING FKM75 62.00 2.50	3	Units	9.50	28.50	
	O-RING FKM75 74.00 3.00	3	Units	11.57	34.71	
	O-RING FKM75 95.00 4.00	12	Units	19.05	228.60	
	O-RING FKM75 100.00 3.00	3	Units	22.39	67.17	
					0	
UO2	Consumables.				386.00	€
	Diesel	20	litres	1.35	27.00	
	Ammonia	2	kg	13.21	26.42	
	Nitrogen	30	litres	3.00	90.00	
	Teflon ring	15	Units	0.30	4.50	
	Electricity	1150	kWh	0.23	264.50	
UO3	Instrumentation.				1598.08	€
	Test-rig	100	h	0.34	34.00	
	Injector holder	1	Units	200.00	200.00	
	Return sleeve	1	Units	70.00	70.00	
	Injector 200um nozzle	1	Units	600.00	600.00	
	Injector 300um nozzle	1	Units	600.00	60.00	
	Data acquisition device YOKOGAWA	56	h	1.04	58.24	
	Injector control hardware	56	h	0.15	8.40	
	Refrigeration system	56	h	0.49	27.44	
UO4	IT tools.				2395.20	€
	Computer	280	h	0.09	25.20	
	SolidWorks License	1	Unit	1500.00	1500.00	
	MATLAB License	1	Unit	800.00	800.00	
	Microsoft Office License	1	Unit	70.00	70.00	
UO5	Labour.				11431.50	€
	Junior engineer	300	h	18.88	5664.00	
	Chief engineer	100	h	47.50	4750.00	
	Lab technician	50	h	20.35	1017.50	
BUDGET	SUMMARY					
	Concept				Amount	€
	Materials.				455.89	
	Consumables.				386.00	
	Instrumentation.				1598.08	
	IT tools.				2395.20	
	Labour.				11431.50	
	Subtotal				16266.67	€
	General expenses (13%)				2114.67	
	VAT [IVA] (21%)				3416.00	
Total Budget					21266.67	€

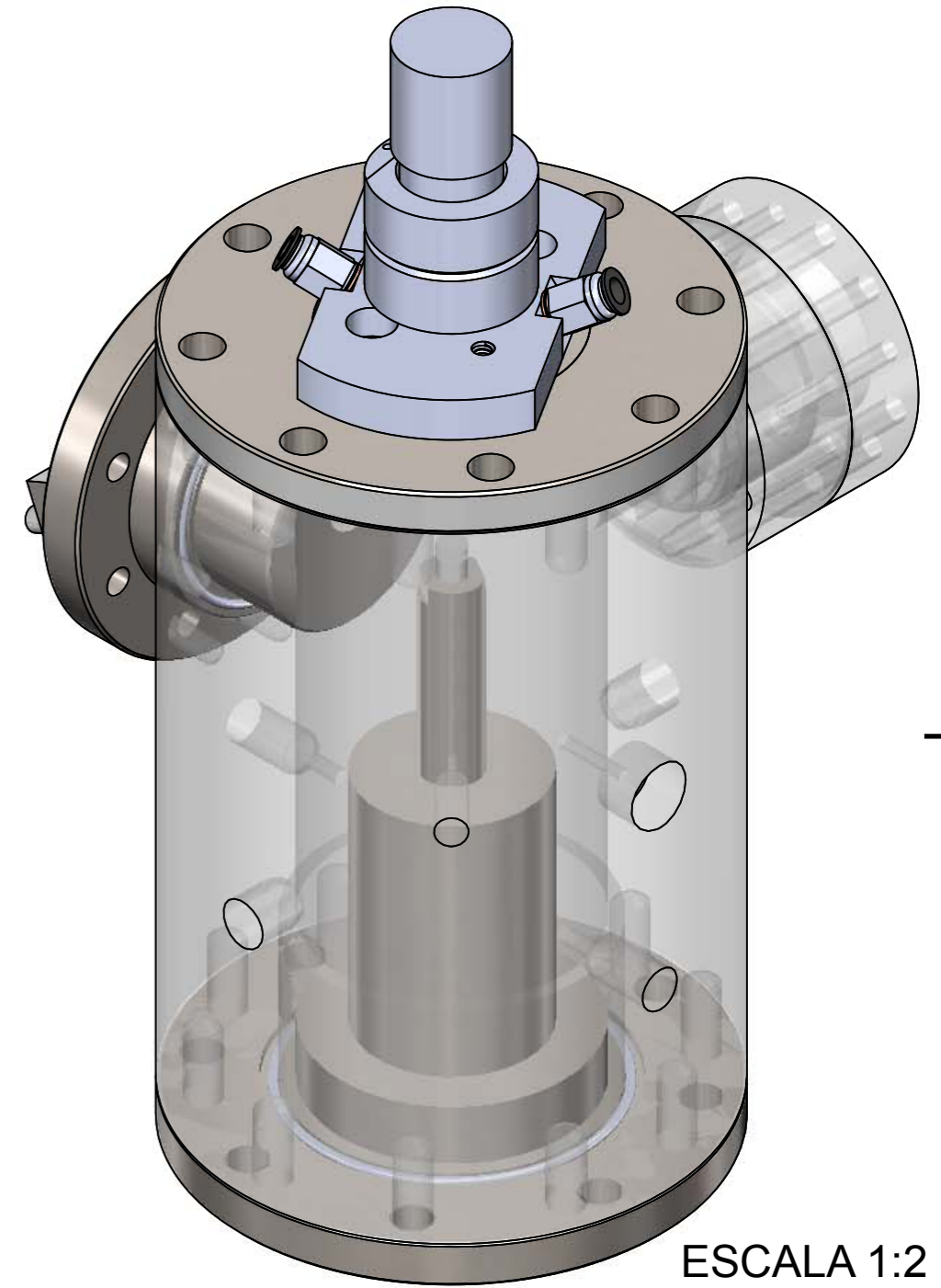
The budget amounts to:
**TWENTY-ONE THOUSAND SEVEN HUNDRED NINETY-SEVEN EUROS
AND THIRTY-FOUR CENTS.**

Part IV

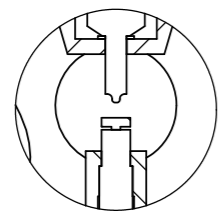
DRAWINGS



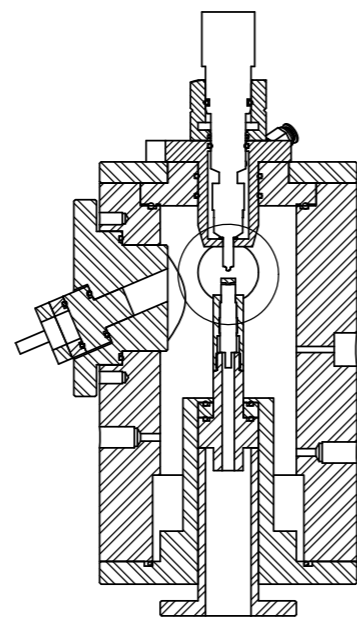
SECCIÓN G-G





ESCALA 1:2



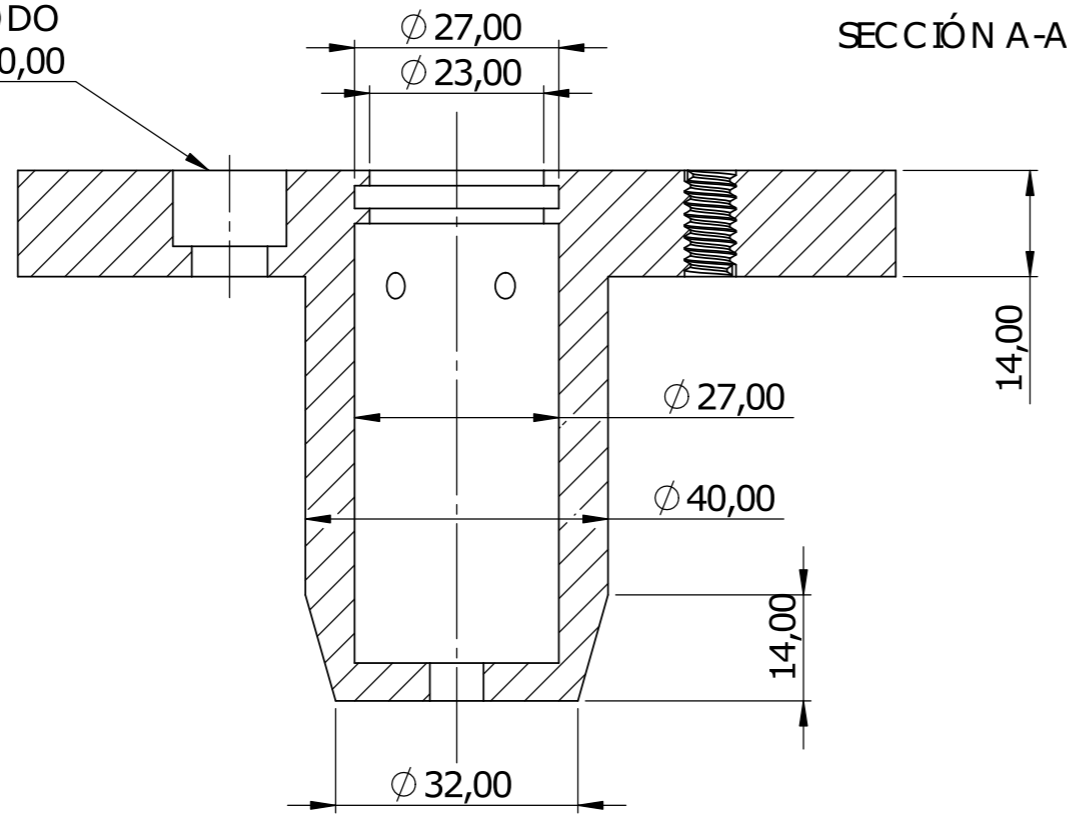
DETALLE C
ESCALA 2:5



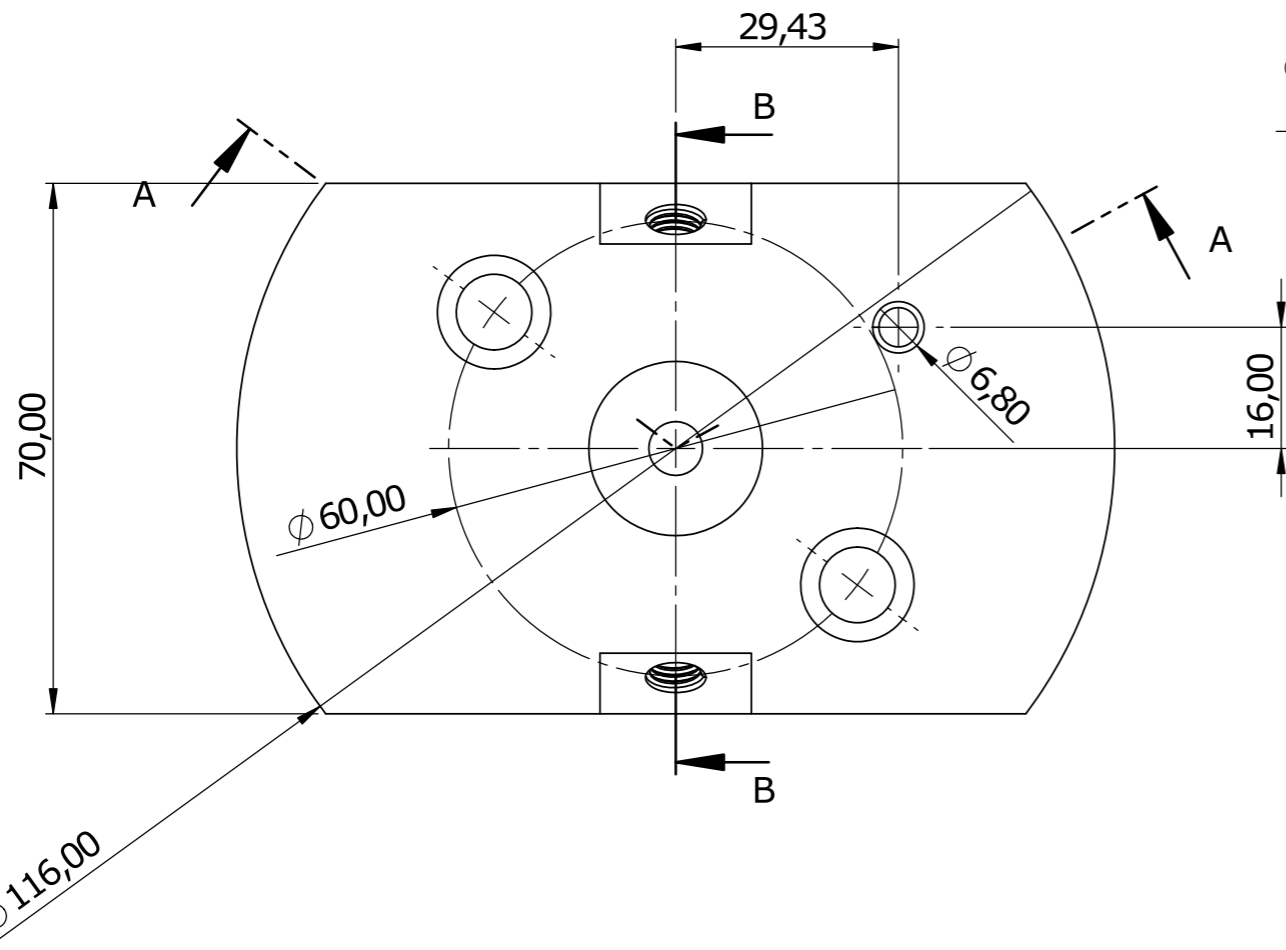
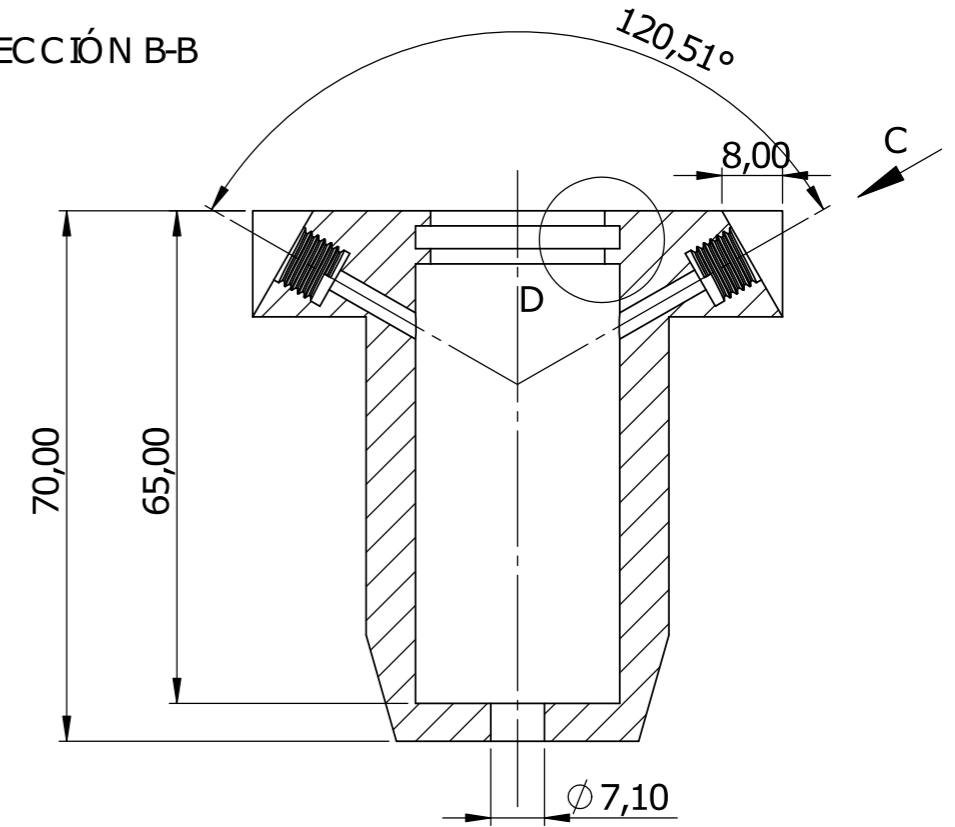
SECCIÓN B-B

 UNIVERSITAT POLITÈCNICA DE VALÈNCIA  <small>Camino de Vera, s/n 46022 Valencia (Spain) Tel: +34 963877650 E-mail: cmt@mot.upv.es</small>	Tipo de documento: Plano de ensamble	Creado por: Omar Cheddadi Rouchi	Fecha: 01/07/2024	
	Si no se especifica lo contrario: Unidades en: mm Tolerancia Linear: ± 0.2 Angular: $\pm 0.2^\circ$ Acabado superficial: N9	Aprobado por: Gabriela Bracho León	01/07/2024	
		CdM Test Rig		
A3 Escala: 1:5	Acabado: Material:	Referencia:	Revisión:	Hoja: 1 of 1

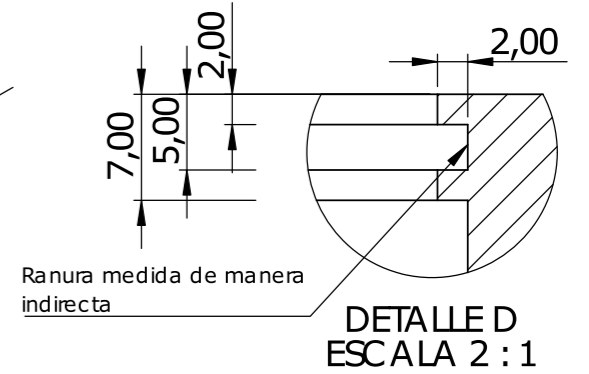
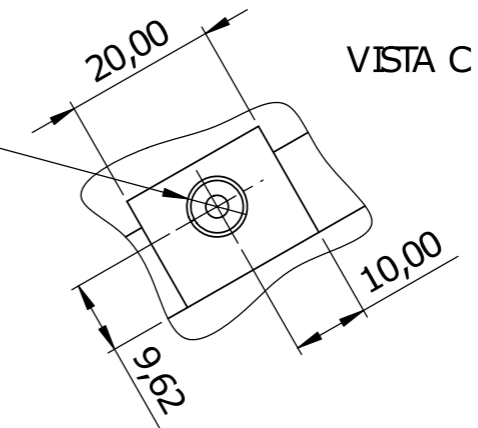
Ø 10,00 POR TODO
 □ Ø 15,00 ∇ 10,00





SECCIÓN B-B



Ø 3,00 POR TODO
 □ M8 ∇ 7,00



 UNIVERSITAT POLITÈCNICA DE VALÈNCIA  Camino de Vera, s/n 46022 Valencia (Spain) Tel: +34 963877650 E-mail: cmt@mot.upv.es	Tipo de documento: Plano de componente	Creado por: Omar Cheddadi Rouchi	Fecha: 01/07/2024
	Si no se especifica lo contrario: Unidades en: MM Tolerancia Lineal: ±0.2 Angular: ±0.2° Acabado superficial: N9	Aprobado por: Gabriela Bracho León	01/07/2024
Acabado:	Material: Acero INOX AISI 316	Referencia: Portinyector refrigerado	Revisión: Hoja: 1 of 1

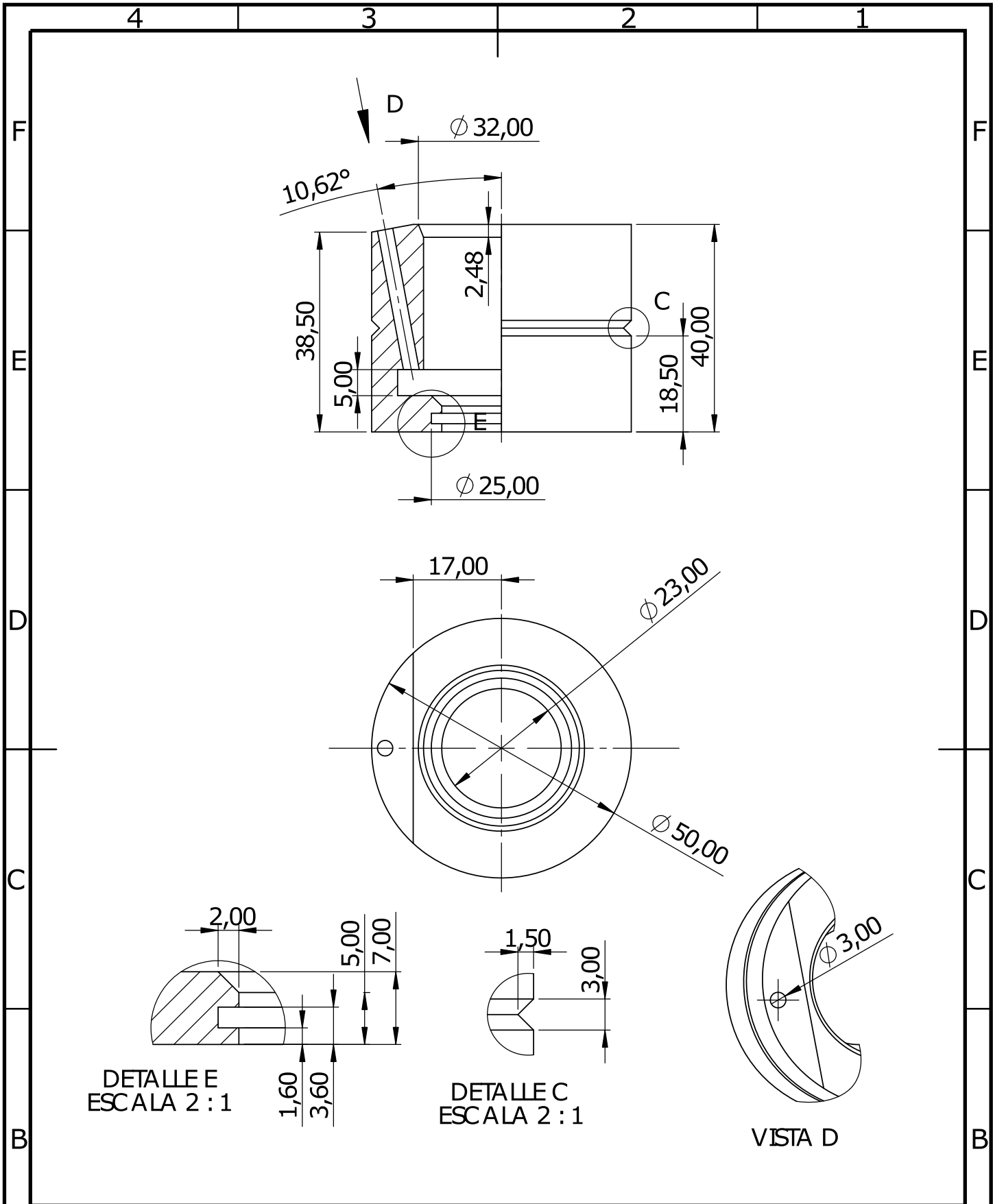
A3

Escala: 1:1

Acero INOX AISI 316

Portinyector refrigerado

Revisión: Hoja:
1 of 1



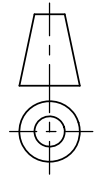
DETALLE E
ESCALA 2 : 1

DETALLE C
ESCALA 2 : 1

VISTA D



Camino de Vera, s/n 46022 Valencia (Spain)
Tel: +34 963877650 E-mail: cmt@mot.upv.es



Tipo de documento:
Plano de pieza

Si no se especifica lo contrario:
Unidades en: mm
Tolerancia
Linear: ± 0.2 Angular: $\pm 0.2^\circ$
Acabado superficial: N9

Creado por:
Omar Cheddadi Rouchi Fecha: **26/06/2024**

Aprobado por:
Gabriela Bracho León Fecha: **28/06/2024**

Description:
Camisa retorno inyector

A4 Escala: **1:1**

Acabado:
Material:

Referencia:
Revisión:
Hoja: **1 of 1**

1

2

3

4

A

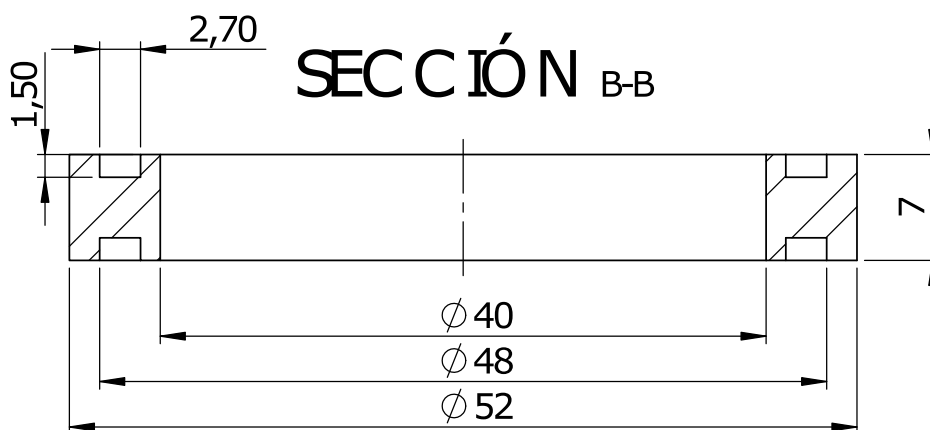
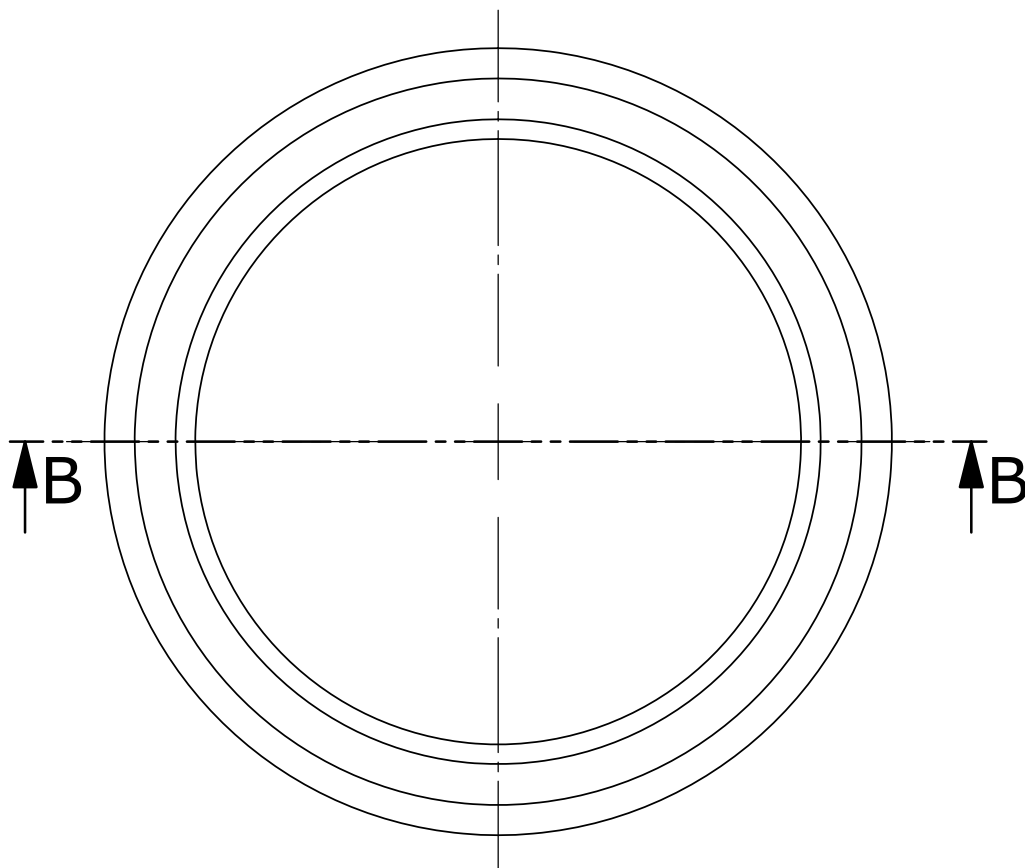
B

C

D

E

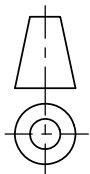
F



UNIVERSITAT
POLITÈCNICA
DE VALÈNCIA



Camino de Vera, s/n 46022 Valencia (Spain)
Tel: +34 963877650 E-mail: cmt@mot.upv.es



Tipo de documento:

Plano de pieza

Si no se especifica lo contrario:

Unidades en: mm

Tolerancia

Linear: ± 0.2 Angular: $\pm 0.2^\circ$

Acabado superficial: N9

Creado por:

Omar Cheddadi Rouchi

Fecha:

26/06/2024

Aprobado por:

Gabriela Bracho León

28/06/2024

Description:

Anillo separacion inyector

Acabado:

Material:

Acero Inox. AISI 316

Referencia:

Revisión:

Hoja:

A4

Escala: **2:1**

1 of 1